High frequency neuronal bursting is essential for circadian and sleep behaviors in *Drosophila*

Florencia Fernandez-Chiappe[1¶], Lia Frenkel[2,3¶], Carina Celeste Colque[2], Ana Ricciuti[1], Bryan Hahm[1], Karina Cerredo[1], Nara Inés Muraro[1,2*] and María Fernanda Ceriani[2*]

[1] Current address: Instituto de Investigación en Biomedicina de Buenos Aires (IBioBA) - CONICET - Partner Institute of the Max Planck Society, Buenos Aires, Argentina.

[2] Fundación Instituto Leloir - IIBBA - CONICET, Buenos Aires, Argentina.

[3] Instituto de Biociencias, Biotecnologías y Biomedicina (IB3) - Departamento de Fisiología Biología Molecular y Celular - Facultad de Ciencias Exactas y Naturales - Universidad de Buenos Aires, Buenos Aires, Argentina.

[¶] These authors contributed equally to this work.

[*] Shared corresponding authors.

Correspondence: nmuraro@ibioba-mpsp-conicet.gov.ar, fceriani@leloir.org.ar

Short Title: I_h channel in fly circadian and sleep behaviors

Abstract

Circadian rhythms have been extensively studied in *Drosophila*, however, still little is known about how the electrical properties of clock neurons are specified. We have performed a behavioral genetic screen through the downregulation of candidate ion channels in the lateral ventral neurons (LNvs) and show that the hyperpolarization-activated cation current I_h is important for the behaviors that the LNvs command: temporal organization of locomotor activity and sleep. Using whole-cell patch clamp electrophysiology we demonstrate that small LNvs are bursting neurons, and that I_h is necessary to achieve the high frequency bursting firing pattern characteristic of both types of LNvs. Since firing in bursts has been associated to neuropeptide release, we hypothesized that I_h would be important for LNvs communication. Indeed, herein we demonstrate that I_h is fundamental for the recruitment of PDF filled dense core vesicles to the terminals at the dorsal protocerebrum and for their timed release, and hence for the temporal coordination of circadian behaviors.

Introduction

Circadian (*circa*: around, *diem*: day) rhythms are biological rhythms with a period of approximately 24h that have evolved in essentially all organisms. They confer an important adaptive value by allowing the anticipation to the daily changes in environmental conditions associated to the rotation of our planet. The “around the clock” coordination of behavior and physiology in *Drosophila* is regulated by approximately 150 neurons grouped in different clusters and named after their anatomical localization (1). Among them, the small lateral ventral neurons (sLNvs) have been identified as a fundamental group in the control of behavioral rhythms under free running conditions, communicating via the release of the neuropeptide Pigment Dispersing Factor (PDF) (2-5) and glycine (6). The large lateral ventral neurons (lLNvs), on the other hand, are highly relevant for arousal and the PDF they release provides wake promoting functions (7-9).

Although the mechanisms that give rise to the cell-autonomous cycling of gene and protein expression and comprise the core of the molecular clock have been described thoroughly (10), one of the challenges of the field now is to understand how different clock neurons communicate to each other. It is indeed the emerging properties of these clock neuronal circuits acting concertedly that provide the system with plasticity and adaptability (11). But to understand the communication taking place within clock neurons, it is paramount to examine the physiological properties of the different neuronal groups. The type, amount and distribution of ion channels

present in the membrane of a neuron determine features such as excitability and action potential firing pattern. In particular, clock neurons change their electrical activity on a daily basis, with higher action potential firing during the day than at night, a phenomenon that has been described both in mammals and flies (reviewed in (12).

In *Drosophila*, several ion channels have already been found to play roles in different aspects of circadian function, such as the calcium dependent voltage-gated potassium channel *slowpoke* (*slo*) (13, 14) and its binding protein (*slob*) (13, 15, 16), the cation channel *narrow abdomen* (*na*) (17-19), the voltage-gated potassium channel *Shaw* (20, 21), the inward rectifying potassium channel *Ir* (22), the temperature sensitive *trpA1* channel (23), the potassium channel *hyperkinetic* (*hk*) (24) and the voltage-gated potassium channel *Shal* (21, 25). Under the hypothesis that additional ion channels are involved in determining the characteristic physiological properties of the LNvs that ensure circadian organization of locomotor activity, we performed a behavioral genetic screen downregulating candidate ion channels using RNA interference (RNAi) specifically in LNvs. Following this strategy, we have been able to identify several ion channels that, when knocked down, alter circadian locomotor behavior under free running conditions. Of those, we have first focused our attention on the hyperpolarization-activated cation current $I_{h,}$ since, as it has been described in mammalian neurons (26), its biophysical properties make it particularly suitable to mediate the organization of action potential firing in bursts, a firing mode that characterizes lLNvs (27-29) and, we show here, also sLNvs. Consistently, we demonstrate that perturbing I_h causes a decrease in the frequency of LNvs bursting that is accompanied by a reduction in PDF immunoreactivity and in the complexity of sLNv axonal termini. Moreover, we have found that the disruption of I_h is accompanied by an increase in sleep. Altogether, our results reveal a novel function of I_h in determining LNvs physiology and the behaviors they command, and uncover several additional ion channels with putative roles in these important clock clusters, for future exploration.

Results

LNvs ion channel downregulation behavioral screen

To shed light onto how LNvs achieve the physiological properties that allow them to play a key role in the circadian organization of locomotor activity, we performed an ion channel downregulation behavioral screen. The *pdf*-Gal4 driver, in the presence of UAS-*dicer2* (from here on *pdf,dicer*) was used to drive expression of UAS-RNAis to knock down the expression of

candidate ion conductances solely in LNvs. The RNAis were chosen to target ion channel genes, genes coding for ion channel auxiliary subunits or genes coding for ion channel transporters which had not been reported to be involved in LNvs-driven circadian phenotypes before. The locomotor activity of *pdf,dicer*>RNAi male flies was recorded using *Drosophila* Activity Monitors (DAM, Trikinetics) for 9 days in DD after 3 days of LD entrainment. Each RNAi was initially tested once and, in the case of showing a differential phenotype in DD, corresponding to either a change of circadian period or deconsolidation of locomotor activity, experiments were repeated. In some cases a non-significant trend towards a phenotype was detected and therefore two RNAis that targeted different regions of the same gene were genetically combined to achieve a more potent downregulation. **Table 1** shows the positive hits of our screen, revealing novel ion channels or ion channel auxiliary subunits likely to play roles in LNvs circadian function, namely: *cacophony* (*cac*, CG1522), *Ca-α1T* (*Ca^{2+}-channel protein α_1 subunit T*, CG15899), *ClC-a* (*Chloride channel-a*, CG31116), *CngA* (*Cyclic nucleotide-gated ion channel subunit A*, CG42701), I_h (I_h *channel*, CG8585), *Ork1* (*Open rectifier K^+ channel* 1, CG1615), *Shal* (*Shaker cognate l*, CG9262) and *tipE* (*temperature-induced paralytic E*, CG1232). The RNAis that did not show altered circadian phenotypes in our screen are listed in **S1 Table**. In total 70 RNAis aimed at 36 different genes were tested.

Although all of the ion channel genes that resulted positive hits of our behavioral screen are worth of further assessment, we focused our attention on the hyperpolarization-activated cation current I_h. Little is known about this channel in *Drosophila*, but its homologues in mammals have been implicated in diverse functions such as the generation of pacemaker potentials and the determination of neuronal excitability, among others (26). RNAi-mediated downregulation of I_h in LNvs produced a subtle but consistent decrease in locomotor rhythmicity without altering free running period (**Tables 1 and 2**, **Fig 1A**).

The *pdf*-Gal4 driver used for the ion channel behavioral screen is active throughout development. Therefore, to dissect whether the behavioral phenotype observed was due to a developmental defect or to a post-developmental functional role, we downregulated I_h expression in LNvs in an adult-specific fashion using the GeneSwitch inducible system (30). When the previously reported *pdf*-GeneSwitch (*pdf*GS) driver (31) was utilized to knock down I_h adult-specifically in LNvs, we also observed a decrease in circadian rhythmicity (**Table 2**, **Fig 1B**), indicating that the I_h channel is necessary post-developmentally in LNvs for the maintenance of circadian function. As a complementary approach, we assessed the circadian behavior of previously reported I_h null mutants, I_h^{f01485} and I_h^{f03355} (32, 33). As expected, these mutants also

showed reduced rhythmicity under free running conditions (**Table 2**, **Fig 1C**). Not surprisingly, I_h mutants are less rhythmic than any tissue-specific knock down (LNvs-specific manipulations), strongly suggesting that I_h may be necessary not only in LNvs but also in other neuronal types for the rhythmic organization of locomotor activity under free running conditions. All these genetic manipulations did not, in any case, produce changes in free running period (**Table 2**). To assess if I_h is important for circadian function also under entrained conditions, we analyzed morning and evening anticipatory behavior. Consistent with the strength of the phenotypes observed in DD, we detected a failure in both, morning and evening anticipation in I_h^{f03355} mutants, which is less pronounced in the I_h^{f01485} mutants and the adult-specific downregulation of I_h; no effects were detected under I_h constitutive knock down, suggesting potential compensatory mechanisms (**Table 2**). Taking together, these results suggest that the I_h channel contributes to define the firing properties of neurons controlling circadian behavior.

I_h is necessary for high frequency bursting firing of LNvs

One of the main reasons why we decided to select I_h as the ion channel for in depth analysis is the association of I_h with the organization of action potential firing in bursts. It has been reported, mainly from mammalian thalamic relay and inferior olivary nucleus neurons, that a combination of a hyperpolarization-activated cation current such as I_h, together with a low-voltage activated T-type calcium current (a channel type also uncovered by our screen, **Table 1**), could mediate a bursting firing mode (26). This is because of I_h particular biophysical properties, which opens upon hyperpolarization but carries a depolarizing current (mainly due to the influx of Na^+). This current takes the membrane potential to the activation threshold of the T-type voltage-gated Ca^{++} channel which depolarizes the membrane up to the action potential firing threshold, opening the classical voltage-gated Na^+ channels. Because I_h is slow to close and does not inactivate, the membrane stays in a depolarized state for longer, generating a burst of action potentials. Once I_h closes, the classical voltage-gated K^+ channels that repolarize the membrane, together with the leak K^+ channels, produce the after-hyperpolarization that kick starts the following burst, activating I_h again (26).

Another relevant observation is that firing in bursts is an effective way of releasing neuropeptides, which are stored in dense core vesicles. In contrast to small clear vesicles containing classical fast neurotransmitters, neuropeptide-filled dense core vesicles require a larger amount of Ca^{++} entering the cell to activate the machinery that fuses and releases the dense core

147 vesicles content (reviewed in (34, 35)). Since lLNvs have been described to fire action potentials in
148 a bursting mode (27, 28) and also to be neuropeptide-releasing neurons (2, 36), the hypothesis we
149 formulated is that I_h participates in the active bursting firing mode of LNvs and plays a role in the
150 release of PDF.

151 We first tested our hypothesis in the lLNvs, which have effectively been shown to be
152 bursting neurons (27, 28). We performed *ex vivo* whole-cell current clamp recordings of control
153 *pdf*-RFP (expressing a red fluorofore in the LNvs thus enabling the identification of the two
154 neuronal types due to the difference in the size of their soma) lLNvs and compared their bursting
155 frequency to I_h^{f03355} homozygote mutants. Because we have reported that lLNv bursting frequency
156 also depends on synaptic inputs that are disrupted during the dissection protocol (29) we
157 compared the bursting frequency of control and I_h^{f03355} mutant lLNvs at exactly the same time
158 post-dissection (23 minutes). **Fig 2A and D** show that although lLNvs from I_h^{f03355} homozygote
159 mutants can still organize their action potential firing in bursts, they do so at a statistically
160 significant lower frequency (mean bursting frequency ± SEM (bursts/min) are
161 $lLNvs_{CONTROL}$=26.2±0.9 and $lLNvs_{Ihf03355}$=17.5±1.4). Other parameters, such as overall firing
162 frequency and membrane potential were not significantly affected in I_h^{f03355} mutants (**S1 Fig A and**
163 **B**).

164 Next, we tested our hypothesis in the sLNvs. Information regarding sLNvs
165 electrophysiological properties is scarce (28, 37), probably due to the technical challenge that their
166 small soma size represents. However, given the important role that sLNvs play in the control of
167 circadian behavior, we analyzed their firing properties in detail. We report here that the sLNvs also
168 fire action potentials organized in bursts (**Fig 2B**). Because obtaining a large amount of recordings
169 in whole-cell configuration was a difficult task to achieve, we recorded action potential firing rate
170 and bursting frequency in a cell-attached configuration of the sLNvs of control (*pdf*-RFP) and I_h^{f03355}
171 homozygote mutants. We found that, similarly to lLNVs, sLNvs show a decreased bursting
172 frequency in the absence of I_h (**Fig 2C and D,** mean bursting frequency ± SEM (bursts/min) are
173 $sLNvs_{CONTROL}$=25.7±1.2 and $sLNvs_{Ihf03355}$=19.3±1.3), without significantly affecting overall firing
174 frequency (**S1 Fig C**).

175 A feature that should be remarked is that both types of LNvs display equivalent basal
176 bursting frequencies (**Fig 2D**), suggesting that this parameter depends on common synaptic inputs
177 and/or shared intrinsic mechanisms. We have previously reported that lLNvs bursting frequency
178 relies to some extent on synaptic inputs coming from the visual neuropiles, which indirectly

involve L2 lamina neurons and the neurotransmitter acetylcholine (29). The dependence of lLNv bursting on these synaptic inputs is illustrated by the fact that this parameter decays as a function of the time elapsed since brain dissection, which removes the retina (29). We found that sLNv bursting frequency also decays with time *ex vivo*, which can be seen both at the population level (**S2 Fig A**) and also in individual cells (**S2 Fig B-C**), suggesting that both types of LNvs depend on synaptic inputs which are gradually lost after dissection. Alternatively, it might be that lLNvs rely on visual circuit inputs to burst, and sLNv bursting depends on lLNv bursting. Certainly, the neuronal processes of lLNvs are better localized, spanning all over the optic lobes, to integrate visual information. However, the sLNvs have been shown to receive direct input from the Hofbauer-Buchner (HB) eyelet extraretinal organ (38), whose integrity may also be compromised during dissection. Whether sLNvs and lLNvs rely on different or similar synaptic inputs to support bursting frequency, or if one LNv group depends on the other to detect synaptic information from visual organs, will require further investigation.

We also compared bursting frequency at a different time post-dissection; interestingly, this analysis showed that both large and small LNvs present equivalent bursting frequency, and the lack of I_h produces a significant reduction of this parameter, which is of the same magnitude in the two LNv groups (**S2 Fig D**, compare to Fig 2D, mean bursting frequency ± SEM (bursts/min) are as following $lLNvs_{CONTROL}$=21.0±0.9, $lLNvs_{lhf03355}$=13.8±0.9, $sLNvs_{CONTROL}$=21.1±1.5, $sLNvs_{lhf03355}$=14.6±0.9). Altogether, our results suggest that both LNv clusters share common mechanisms to control their bursting firing frequency, which appear to be controlled intrinsically, likely involving the I_h current, as well as rely on synaptic inputs.

I_h channel and the sLNvs outputs

Over the years it has been demonstrated that communication from the sLNvs to other clock clusters is crucial for coherent circadian behavior under free running conditions (2, 3, 5, 6, 14, 39-41). The rhythmic accumulation of PDF neuropeptide in sLNvs axonal termini has been implicated in this communication, with high immunoreactivity detected in the early morning and low immunoreactivity at night (42). We hypothesized that release of dense core vesicles containing PDF would be affected by the decrease in bursting activity that accompanies I_h downregulation. To test this, we performed anti-PDF immunofluorescence in whole brains of flies with adult-specific downregulation of I_h. **Fig 3A-B** shows that PDF immunoreactivity in controls

(*pdfGS/+*) displays the normal cycling pattern; however, upon downregulation of I_h (in *pdfGS>*I_h^{RNAi}) PDF levels at the axonal termini are constantly reduced and clamped in a night-like state.

In addition to PDF cyclic accumulation, sLNvs show circadian variation of the complexity of their axonal arborizations (43) in order to contact different synaptic targets at different times of the day (44). This structural synaptic plasticity has been shown to be activity-dependent (31, 45, 46), therefore we wondered whether I_h downregulation would affect this property. **Fig 3C-D** shows that total axonal crosses measured by Sholl analysis in controls display the normal cycling pattern, where the terminals are maximally spread (and more complex) in the early morning and less complex at night, where axonal terminals are collapsed together. In contrast, I_h downregulation leads to axonal projections that display little complexity throughout the day, accompanying the reduced PDF levels. Our speculation on why I_h downregulation leaves both, PDF and terminal complexity at levels similar to ZT14 is that I_h underlies high activity bursting firing, a property that is functional during the day. Downregulation of this channel impairs this high frequency bursting that would be associated to increased PDF levels and the spreading of sLNv axonal projections in the morning, both phenomena that have been described to be clock and activity-dependent (31, 45, 46). Moreover, we have previously described that structural plasticity depends on PDF levels (47), so the collapsed state of the projections could be linked to PDF decrease as well. To corroborate whether the defects shown upon I_h downregulation are linked to reduced PDF levels we used the GeneSwitch system to express *pdf* in the context of I_h downregulation. **Fig 4A, C-D** shows that indeed, in the context of a surplus of PDF, cycling of this neuropeptide in the sLNvs axonal terminals is restored, while PDF expression in controls cycles with reduced (yet significant) amplitude.

To investigate whether the decreased PDF levels seen at the dorsal projections are due to decreased PDF production or to a failure to recruit PDF-loaded vesicles (i.e. transport) towards the axonal terminal, we measured PDF levels in the sLNv somas. We analyzed somatic PDF levels (see methods) and found that PDF immunoreactivity cycles in the sLNv somas in a way that resembles its cycling at the axonal terminals, with more PDF during the early morning and less PDF at the beginning of the night (**Fig 4B, E-F**). Interestingly, in the context of I_h downregulation, somatic PDF shows an abnormal accumulation during the night, which could be due to a decreased day-time transport towards the axonal terminals that results in anti-phase cycling of somatic PDF levels. PDF overexpression *per se* increases overall levels, preventing PDF cycling in the somas, albeit not in the terminals. On the other hand, PDF overexpression in the context of I_h knock down does not

242 rescue the night-time abnormal PDF accumulation in the somas, however, it does rescue cycling in
243 the projections (**Fig 4C**).

244 Although PDF overexpression rescues some of the I_h-related phenotypes at the cellular
245 level, it fails to rescue free running behavior (**Fig 4 G-H**). A plausible explanation for this may be
246 that PDF cycling in the terminals, although rescued, still shows reduced amplitude (**Fig 4D**) and
247 may not be enough to synchronize the remaining clusters. Alternatively, I_h downregulation and the
248 associated reduction of bursting frequency may be affecting the release of other neuropeptides or
249 neurotransmitters besides PDF, which might also contribute to the neuronal communication
250 needed to maintain rhythmicity under constant conditions. PDF expression in the context of I_h
251 downregulation subtly shortens the free-running period (**Fig 4H**), which is reminiscent of reduced
252 PDF levels (2), although the underlying mechanisms remain to be explored.

253 Overall, these results indicate that I_h defines an essential property of the sLNvs that
254 ensures proper regulation of neuropeptide levels and structural plasticity, and provide a causal
255 link between the alteration of electrical activity and the disruption of circadian behavior.
256 Moreover, the careful determination of PDF levels in the sLNv somas suggest that in the context of
257 I_h downregulation there is defective PDF transport towards the axonal projections, underscoring
258 that action potential firing is responsible for an active recruitment of dense core vesicles to the
259 terminals.

260

261 **Sleep and the I_h channel**

262 We then examined whether reduction in bursting firing frequency and hence,
263 neuropeptide release, could affect sleep behavior. We first quantified sleep behavior in I_h^{f03355}
264 mutants and found that homozygotes displayed an increase in total sleep, mainly due to a
265 significant rise in the number of sleep bouts, which while shorter in duration did not compensate,
266 and resulted in an increase in total sleep during nighttime. Notably, the increase in sleep was more
267 conspicuous towards the end of the night (**Fig 5A-D, Table 3**). Given the ubiquitous nature of this
268 genetic manipulation we reasoned that the deconsolidated sleep phenotype could arise from the
269 lack of I_h in a plethora of neurons; we therefore continued the analysis using I_h RNAi-mediated
270 downregulation in specific LNv clusters.

271 It has previously been demonstrated a significant role of the lLNvs in arousal, as the PDF
272 released by these neurons works as a strong arousal signal (7-9). We therefore analyzed sleep
273 after acute downregulation of the I_h channel in the lLNvs and other non-circadian peptidergic

neurons (combining the *c929*-Gal4 driver with the TARGET system (48)). Similar to the I_h mutants, these flies exhibited an increase in the number of sleep episodes that resulted in a significant rise in nighttime sleep (**Fig 5 E-H, Table 3**); however the duration of the sleep bouts remains unchanged, indicating that the short sleep bout phenotype observed in I_h mutants must derive from the lack of I_h in neurons not covered by the *c929*-Gal4 driver.

Although PDF released from the sLNvs has not been shown to play an arousal role as the one released by the lLNvs, diverse lines of evidence lend support to the notion that sLNvs can have an impact on sleep behavior (49, 50). To test if I_h from sLNvs had any influence on sleep behavior, we resorted to the sLNv-specific driver R6-Gal4 (51). As a consequence of acute downregulation of the I_h channel in sLNvs, flies showed a robust increase in the amount of sleep, both at daytime and nighttime (**Fig 5 I-L, Table 3**). Surprisingly, this rise in sleep was due to a more consolidated sleep, as the sleep bout number was reduced but episodes lasted longer in the experimental flies compared to the genetic controls. I_h downregulation experiments were also performed constitutively, showing similar tendencies than the acute ones (**Table 3**).

Given that I_h downregulation in both clusters resulted in an increase in sleep with different characteristics, we tested whether I_h downregulation in all PDF-positive neurons would result in an additive effect. However, this was not the case, and concomitant I_h knock down correlates with an increase in sleep of similar magnitude. In fact, in case of constitutive downregulation, no significant differences were identified (**Table 3**). Thus, both groups could be contributing to sleep regulation through different mechanisms/signals that, when impaired at the same time, result in a nonlinear combination of effects. Acute and cell-type specific manipulations of LNvs are therefore required to dissect the control of sleep behavior.

Collectively, our work demonstrates that I_h certainly plays a role in the control of sleep behavior, both on the overall levels and the timing of sleep. Alterations in the timing of sleep is particularly prevalent, highlighted by a recurrent decrease in the latency to the first sleep episode after lights-on observed in the majority of the I_h genetic manipulations (**Table 3**). Further work will be necessary to pinpoint how different neurons recruit I_h to regulate various aspects of their physiology. In particular, the role of neuropeptides in sleep control is widely recognized and involves many neurons throughout the brain. We have initiated here an analysis that includes the sLNvs, the lLNvs+other peptidergic non-circadian neurons and the sLNvs+lLNvs, but it is likely that I_h manipulation will impair neuropeptide trafficking in other sleep-related neurons as well.

Discussion

The physiology of a particular neuron is not regulated by a single ion channel type, but by a complex array of different players; they go from the leak conductances that determine input resistance and resting membrane potential which influence dendritic processes, including summation and propagation of synaptic inputs, to the abundance and quality of voltage-gated ion channels that determine the dynamics of action potential firing, and ultimately dictate the release of classical neurotransmitters and neuropeptides. If we add to this picture the channels that are directly or indirectly activated by ligands we will be able to comprehend, and model, neuronal physiology. We have performed a downregulation screen to describe novel ion channels playing roles in establishing the electrical properties of the LNvs, with the aim of advancing the understanding of LNvs physiology. We focused our attention on I_h, a poorly studied ionic current in *Drosophila*.

Since the discovery of the first hyperpolarization-gated current in cardiac function (52) a great deal of information has been gained about the role of this type of channels in determining the physiology of the mammalian heart and brain (26). An interesting feature of I_h channels is that they are not only sensitive to hyperpolarization, but are also modulated by cyclic nucleotides, hence the name of the channel family HCN (for Hyperpolarization Cyclic Nucleotide-gated). The mammalian genome contains four HCN channel genes HCN1-4, each with specific activation characteristics, distinct but in some cases partially overlapping expression patterns, and different roles in neuronal physiology (53). *Drosophila´*s I_h channel is the sole member of the HCN family in its genome (54), but up to 12 different splice variants can be generated, providing diverse channels with particular biophysical properties (55). A phylogenetic analysis indicates that *Drosophila* I_h (also referred in the literature as DMIH) diverged from a common ancestor before the emergence of the four vertebrate subtypes (56). Interestingly, the domain organization of I_h is similar to its vertebrate counterparts, and the interaction between domains is conserved to the point that domain swapping between *Drosophila* I_h and vertebrate HCN channels produce similar biophysical results (57).

Drosophila I_h has not been explored in depth yet but it has been reported in the visual system where it regulates the release of glutamate from amacrine cells (33), and at the larval neuromuscular junction where it affects neurotransmitter release (58). An analysis of I_h mutants shows that this channel controls a variety of behaviors (32). Particularly relevant for our work is the fact that I_h has been reported to control circadian rhythms and sleep in *Drosophila* by acting on

dopaminergic neurons (59). Although Gonzalo-Gomez *et al.* (2012) did not find any PDF disruptions in the sLNvs of the I_h mutants they generated, our current analysis of adult-specific downregulation of I_h shows that it does affect PDF levels and the structural plasticity at the sLNvs dorsal projections, as well as the accumulation of PDF in the somas albeit with altered circadian dynamics. This highlights the importance of using strategies where a genetic manipulation is performed acutely, in order to avoid homeostatic compensations that may conceal a phenotype. Altogether the collective evidence indicates that I_h may be modulating circadian rhythms and sleep by exerting its role in more than one neuronal type. Whether the molecular mechanisms that regulate, and are regulated by I_h in LNvs and in dopaminergic neurons are similar will require further examination.

Sleep behavior has been previously reported in I_h mutant flies, and, taking into account our contribution, the accumulated evidence raises some controversy that deserves special attention. Using an independently generated I_h null mutant, Gonzalo-Gomez *et al*. (2012) reported that total sleep was unchanged; but they showed, similar to our results, a deconsolidation of sleep resulting from an increase in sleep bout number of shorter duration (59). On the other hand, during the initial characterization of the mutants used in our study, Chen *et al.* reported the opposite sleep phenotype, that is, a decrease in total sleep, with no changes in bout number (32). One important element to take into account is that I_h mutant flies are hyperactive (**Table 3**) and therefore inferring sleep from activity data should be approached with caution. Since I_h mutants display an increase in sleep, and hyperactivity would result in an underestimation of sleep, our results are validated. It is not uncommon to come across published fly sleep data inferred from activity monitoring where basal activity is not reported (32), a practice that warrants further attention.

Perhaps more informative than the mutants is our sleep analysis following acute and cluster-specific downregulation of I_h. We show here that *c929*+ peptidergic neurons use I_h to promote arousal, which in the case of the lLNvs would likely be mediated by PDF release following high frequency neuronal bursting. However, the release of other neuropeptides could also be affected by I_h downregulation; in fact additional neurons besides lLNvs contribute to the waking state within the *c929*-Gal4 driven group (8). Moreover, specific downregulation of I_h in the sLNvs also results in an increase of sleep, however, this increase corresponds to a more consolidated sleep and therefore, although an increase in total sleep is produced upon I_h downregulation with both R6-Gal4 and *c929*-Gal4, the properties of these sleep increase are different. This may indicate

that, either the neuropeptide/s these neuronal clusters are releasing with the help of I_h, or the effects these signals are conveying to their particular postsynaptic targets, are probably different. These findings should be thoroughly characterized in the future, as they provide clear evidence of the participation of the sLNvs in the neuronal circuits governing sleep. Interestingly, in a recent genome-wide association study, ion channels were one of the two main pathways associated to sleep duration both in humans and flies, indicating an evolutionarily conserved function of ion channels in regulating a complex behavior such as sleep (60).

Although no role has been directly demonstrated for I_h in *Drosophila* clock neurons before our work, the HCN family has been proposed to contribute to the circadian variations in neuronal excitability in the mammalian suprachiasmatic nucleus (SCN) (61). HCN channels have been reported to be expressed in the SCN (62) but their function has been difficult to discern due to a lack of strong and significant phenotypes following genetic and pharmacologic manipulations, which could be due to the heterogeneity of the SCN neuronal population and the genetic compensation that may arise from having several HCN channel genes (63-65). Taking advantage of the fact that *Drosophila* clock neuron clusters are well identifiable, and that there is only one member of the HCN channel family, we were able to show that I_h is a crucial player defining the high activity bursting physiology of LNvs, and that this regulates neuronal outputs and behavior.

The role of cyclic nucleotide cascades in LNvs has been mainly focused on their capacity as transducers of information that impacts on gene expression in the context of the regulation of the circadian clock (66, 67). Our screen has uncovered two cyclic nucleotide-modulated channels (I_h and CngA), suggesting that the integration of information signaled by cyclic nucleotides is crucial for circadian function also at rapid time frames, a hypothesis that has already been proposed (67, 68). The case of I_h, being modulated by both hyperpolarizing voltage and cyclic nucleotides, provides additional complexity, as they could serve as coincidence detectors (scheme in **Fig 6**). The biophysics of I_h, and therefore the firing properties of LNvs, are affected by both the membrane voltage and the levels of cyclic nucleotides, therefore it is likely that the timing of arrival of these signals may significantly affect the LNvs neuronal output. Albeit purely speculative for the LNvs, the I_h current has been proposed to work as a coincidence detector in other systems (69-71). Further research will be necessary to reveal which are the neuronal inputs that contribute to the hyperpolarization and to the variations of cyclic nucleotide levels. Interestingly, HCN channels have been reported to be activated by Vasoactive Intestinal Peptide (72), which is considered a functional homolog of PDF. Therefore, activation of the PDFR signaling cascade could result in an

increase in cyclic nucleotide (i.e., cAMP) thus modulating I_h, adding players to the already complicated integration of synaptic and cell-autonomous cues coordinated at the sLNvs.

One question that remains to be answered is whether the circadian clock is directly regulating I_h function in LNvs. Although our work has not focused on this issue, a plausible hypothesis is that I_h expression levels may be changing at different times of the day. This is suggested by the work by Abruzzi *et al.* (2011) where they performed chromatin immunoprecipitation tiling array assays with a number of circadian proteins, and showed that the circadian transcription factor CLOCK cycles in its binding to *I_h* regulatory sequences in *Drosophila* heads (73). Among all the positive hits of our screen, I_h is the only one that appears to be directly controlled by the circadian clock according to Abruzzi *et al.* (2011).

Our experiments demonstrate that the sLNvs, considered a central piece of the clock neuron circuitry puzzle, organize their action potential firing in bursts. This bursting frequency depends on synaptic input as it has been shown for the lLNvs (29). LNvs bursting frequency seems to be also influenced by cell autonomous mechanisms since, as we demonstrate here, a null mutation in *I_h* produces a decrease in this parameter. Interestingly, the mutation produces a decrease that is of the same magnitude in sLNvs and lLNvs, suggesting that this ion channel regulates bursting frequency in comparable ways in both neuronal types. Remarkably, the DN1 clock neuron cluster has recently been shown to fire action potentials in bursts and that this temporal coding, i.e. the timing of spiking, is relevant for the control of sleep behavior (16).

The importance of gaining as much information as possible about the I_h current is underscored by the discovery of several I_h channelopathies. Information from both, patients and genetic animal models, has brought to light the relation of mutations on *HCN* channel genes, or accessory subunits, to different conditions such as of epilepsies, autism spectrum disorders, neuropathic pain, Parkinson's disease, depression and cardiac dysfunction among others (74-76). In this context, learning about *Drosophila* I_h helps understanding the basic characteristics of this current and *Drosophila*, with its less complex genome and fantastic genetic amenability, could serve in the future as a model organism to discover interacting proteins and pathways, to ultimately unravel the underlying pathological mechanisms of I_h channelopathies.

Materials and Methods

Fly Strains

All fly strains used in this study are detailed in **S2 Table**. UAS lines for RNAi downregulation of candidate ion channels were obtained from the Bloomington Stock Center (the ones associated to the *Drosophila* RNAi Screening Center, DRSC), from the Vienna *Drosophila* Resource Center (VDRC) and from the National Institute of Genetics Fly Stock Center (NIG). Information for each of these lines is also available in Table 1 (for the positive hits of the genetic screen) and in S1 Table (for the negative hits). Flies were grown and maintained at 25°C in standard cornmeal medium under 12:12h light:dark cycles unless stated otherwise. For experiments involving the adult-specific GeneSwitch expression system, 2-4 day old adult males raised in normal cornmeal food were transferred to food containing RU486 (mifepristone, Sigma) in 80% ethanol to a final concentration 200 µg/ml or with the same amount of ethanol (vehicle) in control treatments. These experiments were done with a line that includes a UAS-CD8::GFP transgene on the II chromosome. For experiments involving the TARGET system (48) flies were raised at 21°C, induction of the expression system was achieved by increasing the temperature to 30°C. Newly eclosed males were used for all circadian rhythmicity experiments, 3-7 day-old non-virgin females were used for sleep and electrophysiology experiments, a mix of males and females was used for immunofluorescence determination.

Locomotor Behavior Analysis

Flies were entrained to 12:12h light:dark cycles during their entire development, and newly eclosed adult males were placed in 65 x 5 mm glass tubes and monitored for activity with infrared detectors and a computerized data collection system (Trikinetics, Waltham, MA). For experiments involving the GeneSwitch expression system, newly eclosed adult males were placed in glass tubes containing standard food (supplemented with 200 mg/ml RU486 or vehicle, as indicated) and monitored for activity. Activity was monitored in LD conditions for 3-4 days, followed by constant darkness for at least nine days (DD1–9). Period and rhythmicity parameters as FFT and power were estimated using ClockLab software (Actimetrics). Flies with a single peak over the significance line ($p<0.05$) in a χ^2 analysis were scored as rhythmic, which was confirmed by visual inspection of the actograms. For LD anticipatory analysis, the last day before switching to DD was used. Average activity plots at the population level were produced using the Clocklab average activity function for each animal, relativized to its own activity, integrated in 30 minutes bins and then the population average for each genotype was calculated. Morning Anticipation Index (MAI) was calculated as follow, the sum of relativized activity from ZT21.5 from the previous day to ZT0 was

465 divided by the sum of relativized activity from ZT19 from the previous day to ZT0 for each animal.
466 Since data was not normally distributed a non-parametric ANOVA analysis, Kruskal-Wallis test
467 followed by Dunn´s multiple was used to test statistically significant differences. An equivalent
468 procedure was performed for the Evening Anticipation Index (EAI) using data from ZT7 to ZT12.
469
470 ***Sleep Behavior Analysis***
471 Female flies were socially housed in vials from eclosion at 25°C under 12:12h light:dark cycles until
472 they were 4 to 6 days-old and afterwards transferred to 65 x 5 mm glass tubes (Trikinetics,
473 Waltham, MA) containing normal cornmeal food. Tubes were loaded onto DAM monitors and
474 locomotor activity was assessed using the DAM system under 12:12h light:dark cycles. Sleep data
475 was calculated on the second day after fly loading into tubes to allow them to recover from
476 anesthesia and to acclimate to the new environment. For experiments using the TARGET system
477 (77) flies were raised at 21°C, socially housed in vials from eclosion until they were 6 days-old and
478 afterwards transferred to 65 x 5 mm glass tubes. Monitors were kept for two days at 21°C to
479 measure sleep under the restrictive temperature at which the RNAi is not expressed (which in all
480 cases produced no effect), and then the incubator temperature was raised to 30°C for two more
481 days to allow RNAi expression, always under 12:12h light:dark cycles. Sleep data was calculated on
482 the second day at 30°C. The DAM System binning time was set to 1min. Sleep was defined as no
483 movement for 5min (78, 79). Rethomics, a collection of packages running in R language (80), was
484 used to infer sleep from locomotor activity data, to build graphs of sleep for 30min as a function of
485 the time of day, to get measurements of total sleep, day sleep, night sleep, sleep bout duration,
486 sleep bout number, latencies to lights on and off and to get an activity index (defined as the
487 average activity counts in the active minutes) of each individual fly. Behavioral experiments were
488 conducted at least 2-3 times, with 15 to 30 individuals per genotype.
489
490 ***Electrophysiology***
491 Three to seven days-old female flies were anesthetized with a brief incubation of the vial on ice,
492 brain dissection was performed on external recording solution which consisted of (in mM): 101
493 NaCl, 3 KCl, 1 $CaCl_2$, 4 $MgCl_2$, 1.25 NaH_2PO_4, 5 glucose, and 20.7 $NaHCO_3$, pH 7.2, with an
494 osmolarity of 250 mmol/kg (based on solution used by Cao and Nitabach, 2008). After removal of
495 the proboscis, air sacks and head cuticle, the brain was routinely glued ventral side up to a sylgard-
496 coated coverslip using a few µls of tissue adhesive 3M Vetbond. The time from anesthesia to the

497 establishment of the first successful recording was approximately 15-19min spent as following: 5-
498 6min for the dissection, 4-5min for the protease treatment to remove the brain's superficial glia
499 and 6-8min to fill and load the recording electrode onto the pipette holder, approach the cell,
500 achieve the gigaohm seal and open the cell into whole-cell configuration to start recording. LNvs
501 were visualized by red fluorescence in *pdf*-RFP using a Leica DM LFS upright microscope with 63X
502 water-immersion lens and TK-LED illumination system (TOLKET S.R.L, Argentina). Once the
503 fluorescent cells were identified, cells were visualized under IR-DIC using a Hamamatsu ORCA-ER
504 camera and Micro Manager software. lLNvs were distinguished from sLNvs by their size and
505 anatomical position. To allow the access of the recording electrode, the superficial glia directly
506 adjacent to LNvs somas was locally digested with protease XIV solution (10mg/ml, SIGMA-ALDRICH
507 P5147) dissolved in external recording solution. This was achieved using a large opened tip
508 (approximately 20μm) glass capillary (pulled from glass of the type GC100TF-10; Harvard
509 Apparatus, UK) and gentle massage of the superficial glia with mouth suction to render the
510 underling cell bodies accessible for the recording electrode with minimum disruption of the
511 neuronal circuits. After this procedure, protease solution was quickly washed by perfusion of
512 external solution. Recordings were performed using thick-walled borosilicate glass pipettes
513 (GC100F-10; Harvard Apparatus, UK) pulled to 6-7 MΩ using a horizontal puller P-1000 (Sutter
514 Instruments, US) and fire polished to 9-12 MΩ. Recordings were made using an Axopatch 200B
515 amplifier controlled by pClamp 9.0 software via a Digidata 1322A analog-to-digital converter
516 (Molecular Devices, US). Recording pipettes were filled with internal solution containing (in mM):
517 102 potassium gluconate, 17 NaCl, 0.085 $CaCl_2$, 0.94 EGTA and 8.5 HEPES, pH 7.2 with an
518 osmolarity of 235 mmol/kg (based on the solution employed by Cao and Nitabach, 2008). Cell-
519 attached configuration was achieved by gentle suction and recordings were performed in voltage-
520 clamp mode with no hold. For whole-cell configuration, gigaohm seals were accomplished using
521 minimal suction followed by break-in into whole-cell configuration using gentle suction in voltage-
522 clamp mode with a holding voltage of -60mV. Gain of the amplifier was set to 1 during recordings
523 and a 5kHz Lowpass Bessel filter was applied throughout. Spontaneous firing was recorded in
524 current clamp (I=0) mode. Analysis of traces was carried out using Clampfit 10.4 software. Bursting
525 frequency was calculated as the number of bursts in a minute of recording. For comparisons, all
526 recordings were quantified at the same time post-dissection as specified in the text and figure
527 legends. For AP firing rate calculation the event detection tool of Clampfit 10.4 was used. In many
528 cases we were able to see the two different AP sizes reported previously (28), however, for AP

529 firing rate calculation only the large APs were taken into account. Traces shown in figures were
530 filtered offline using a lowpass boxcar filter with smoothing points set to 9. Perfusion of external
531 saline in the recording chamber was achieved using a peristaltic pump (MasterFlex C/L). All
532 recordings were performed during the light phase, between ZT1 and ZT10.
533
534 ***Immunofluorescence detection***
535 Heads were cut at *zeitgeber* times 2 and 14, fixed in paraformaldehyde 4% in PB 0.1M for 35-45
536 minutes at room temperature and brains were dissected afterwards, washed 5 times in PBS-Triton
537 X-100 0.1%, blocked with 7% normal goat serum for 2 hours at RT and incubated with primary
538 antibody (see antibodies information in **S2 Table**), ON at 4ºC. After five 15 minutes washes in PBS-
539 Triton X-100 0.1%, brains were incubated with the secondary antibody. Confocal images were
540 obtained in a Zeiss 710 Confocal Microscope or Pascal Confocal Microscope. All the photographs
541 within the same experiment were taken with the same confocal parameters. In the *pdf*
542 overexpression experiments (Fig 4), data was relativized to the average of intensities for each
543 experiment because two different microscopes were used. The acquisition of sLNv soma images
544 required different confocal parameters (laser intensity, gain, zoom).
545
546 ***PDF quantitation***
547 For the quantitation of PDF intensity at the sLNv projections, we assembled a maximum intensity
548 z-stack that contains the whole projection (approximate 10 images) and constructed a threshold
549 image to create a ROI for measure immunoreactivity intensity using ImageJ (NIH). Data was
550 analyzed with InfoStat software (Universidad Nacional de Córdoba, Argentina) and GraphPad. For
551 quantitation of PDF intensity at the sLNv somas we used a unique 1 µm image per cell, which was
552 the one where the PDF cytoplasm immunoreactivity signal could be clearly differentiated from the
553 empty nucleus. The draw tool from ImageJ (NIH) enabled to measure only the PDF signal at the
554 cytoplasm, and this procedure was repeated for each cell (3-4) in each brain (only one brain
555 hemisphere). Background intensity was subtracted for each brain and average intensity was
556 calculated. Data was normalized using the average intensity for the whole population of brains of
557 the experiment. This way of quantifying PDF in the sLNvs somas allowed a more precise
558 assessment of neuropeptide levels and it may be the reason why we were able to detect circadian
559 cycling of PDF levels, unlike previous reports that were unable to detect them (42). Statistics
560 analysis was done using the GraphPad program, after testing data normality one-way ANOVA and

Sidak's multiple comparisons tests were performed to determine time of -day- genotype differences.

Analysis of structural plasticity

To assess the degree of complexity within the sLNvs dorsal projections we performed immunofluorescence against a membrane version of GFP. The maximum intensity z-stack image was transformed into a threshold image and Sholl analysis was performed with ImageJ (NIH) software. Each picture was corroborated by visual inspection to confirm the number of crosses in every 10 µm-concentric Sholl ring. Data was analyzed by means of InfoStat software (Universidad Nacional de Córdoba, Argentina).

Statistical Analysis

The following statistical analyses were used in this study: one-way ANOVA and two-way ANOVA with post hoc Tukey's HSD test for multiple comparisons of parametric data, and non-parametric Kruskal-Wallis statistical analysis with multiple comparisons (p adjustment method = BH) as specified in figure legends. Parametric tests were used when data were normally distributed and showed homogeneity of variance, tested by Kolmogorov Smirnov test and Levene's test, respectively. Sidak's and Dunn's multiple comparisons tests were performed after parametric and non-parametric ANOVA when GraphPad software was used. Sleep data tended to not show a normal distribution, hence non-parametric statistics were used. Statistical analyses were performed using Infostat for circadian rhythmicity and immunofluorescence experiments, R-based Rethomics package for sleep data and Origin software for electrophysiological parameters. A p value < 0.05 was considered statistically significant. Throughout the manuscript n represents the total number of measurements compared in each experimental group (behavior of an individual, brain morphology, or neuronal recordings, depending of the experiment), and N represents the number of independent times an experiment was repeated. Boxes in box and whisker plots for sleep and electrophysiological parameters represent the median and interquartile range (the distance between the first and third quartiles). In all tables, parameters represent the mean value ± standard error of the mean. In dot plots for circadian power and tau and in fluorescence and structural plasticity quantification lines represent the mean value; error bars depict the standard error of the mean.

Acknowledgements

M.F.C., N.I.M. and L.F. are members of the Argentine Research Council for Science and Technology (CONICET). This work was supported by the Agencia Nacional de Promoción Científica y Tecnológica (Grants PICT-2011-2185 to M.F.C. and PICT-2011-2364 and PICT-2015-2557 to N.I.M.), the CONICET (Grant PIP-11220130100378 to N.I.M.) and FOCEM-Mercosur (COF 03/11 to IBioBA). The funders had no role in study design, data collection and analysis, decision to publish, or preparation of the manuscript.Stocks obtained from the Bloomington Drosophila Stock Center (NIH P40OD018537), the NIG-Fly Stock Center and the Vienna Drosophila Resource Center (81) were used in this study. We also thank Dr. Zuo Ren Wang for I_h mutant fly stocks. We thank Esteban Beckwith and Quentin Geissmann for indispensable help with sleep quantification software.

References

1. Yoshii T, Rieger D, Helfrich-Forster C. Two clocks in the brain: an update of the morning and evening oscillator model in Drosophila. Progress in brain research. 2012;199:59-82. Epub 2012/08/11.
2. Renn SC, Park JH, Rosbash M, Hall JC, Taghert PH. A pdf neuropeptide gene mutation and ablation of PDF neurons each cause severe abnormalities of behavioral circadian rhythms in Drosophila. Cell. 1999;99(7):791-802. Epub 2000/01/05.
3. Peng Y, Stoleru D, Levine JD, Hall JC, Rosbash M. Drosophila free-running rhythms require intercellular communication. PLoS biology. 2003;1(1):E13. Epub 2003/09/17.
4. Lin Y, Stormo GD, Taghert PH. The neuropeptide pigment-dispersing factor coordinates pacemaker interactions in the Drosophila circadian system. J Neurosci. 2004;24(36):7951-7. Epub 2004/09/10.
5. Yoshii T, Wulbeck C, Sehadova H, Veleri S, Bichler D, Stanewsky R, et al. The neuropeptide pigment-dispersing factor adjusts period and phase of Drosophila's clock. J Neurosci. 2009;29(8):2597-610. Epub 2009/02/27.
6. Frenkel L, Muraro NI, Beltran Gonzalez AN, Marcora MS, Bernabo G, Hermann-Luibl C, et al. Organization of Circadian Behavior Relies on Glycinergic Transmission. Cell reports. 2017;19(1):72-85. Epub 2017/04/06.
7. Shang Y, Griffith LC, Rosbash M. Light-arousal and circadian photoreception circuits intersect at the large PDF cells of the Drosophila brain. Proceedings of the National Academy of Sciences of the United States of America. 2008;105(50):19587-94.
8. Parisky KM, Agosto J, Pulver SR, Shang Y, Kuklin E, Hodge JJ, et al. PDF cells are a GABA-responsive wake-promoting component of the Drosophila sleep circuit. Neuron. 2008;60(4):672-82. Epub 2008/11/29.
9. Sheeba V, Fogle KJ, Kaneko M, Rashid S, Chou YT, Sharma VK, et al. Large ventral lateral neurons modulate arousal and sleep in Drosophila. Current biology : CB. 2008;18(20):1537-45.
10. Top D, Young MW. Coordination between Differentially Regulated Circadian Clocks Generates Rhythmic Behavior. Cold Spring Harbor perspectives in biology. 2018;10(7). Epub 2017/09/13.
11. Beckwith EJ, Ceriani MF. Communication between circadian clusters: The key to a plastic network. FEBS letters. 2015;589(22):3336-42. Epub 2015/08/25.
12. Allen CN, Nitabach MN, Colwell CS. Membrane Currents, Gene Expression, and Circadian Clocks. Cold Spring Harbor perspectives in biology. 2017;9(5). Epub 2017/03/02.
13. Ceriani MF, Hogenesch JB, Yanovsky M, Panda S, Straume M, Kay SA. Genome-wide expression analysis in Drosophila reveals genes controlling circadian behavior. J Neurosci. 2002;22(21):9305-19. Epub 2002/11/06.

14. Fernandez MP, Chu J, Villella A, Atkinson N, Kay SA, Ceriani MF. Impaired clock output by altered connectivity in the circadian network. Proceedings of the National Academy of Sciences of the United States of America. 2007;104(13):5650-5. Epub 2007/03/21.
15. Jaramillo AM, Zheng X, Zhou Y, Amado DA, Sheldon A, Sehgal A, et al. Pattern of distribution and cycling of SLOB, Slowpoke channel binding protein, in Drosophila. BMC neuroscience. 2004;5:3. Epub 2004/03/10.
16. Tabuchi M, Monaco JD, Duan G, Bell B, Liu S, Liu Q, et al. Clock-Generated Temporal Codes Determine Synaptic Plasticity to Control Sleep. Cell. 2018;175(5):1213-27 e18. Epub 2018/10/16.
17. Nash HA, Scott RL, Lear BC, Allada R. An unusual cation channel mediates photic control of locomotion in Drosophila. Current biology : CB. 2002;12(24):2152-8. Epub 2002/12/25.
18. Lear BC, Lin JM, Keath JR, McGill JJ, Raman IM, Allada R. The ion channel narrow abdomen is critical for neural output of the Drosophila circadian pacemaker. Neuron. 2005;48(6):965-76. Epub 2005/12/21.
19. Flourakis M, Kula-Eversole E, Hutchison AL, Han TH, Aranda K, Moose DL, et al. A Conserved Bicycle Model for Circadian Clock Control of Membrane Excitability. Cell. 2015;162(4):836-48. Epub 2015/08/16.
20. Hodge JJ, Stanewsky R. Function of the Shaw potassium channel within the Drosophila circadian clock. PloS one. 2008;3(5):e2274. Epub 2008/05/30.
21. Smith P, Buhl E, Tsaneva-Atanasova K, Hodge JJL. Shaw and Shal voltage-gated potassium channels mediate circadian changes in Drosophila clock neuron excitability. The Journal of physiology. 2019;597(23):5707-22. Epub 2019/10/16.
22. Ruben M, Drapeau MD, Mizrak D, Blau J. A mechanism for circadian control of pacemaker neuron excitability. Journal of biological rhythms. 2012;27(5):353-64.
23. Lee Y, Montell C. Drosophila TRPA1 functions in temperature control of circadian rhythm in pacemaker neurons. J Neurosci. 2013;33(16):6716-25. Epub 2013/04/19.
24. Fogle KJ, Baik LS, Houl JH, Tran TT, Roberts L, Dahm NA, et al. CRYPTOCHROME-mediated phototransduction by modulation of the potassium ion channel beta-subunit redox sensor. Proceedings of the National Academy of Sciences of the United States of America. 2015;112(7):2245-50. Epub 2015/02/04.
25. Feng G, Zhang J, Li M, Shao L, Yang L, Song Q, et al. Control of Sleep Onset by Shal/Kv4 Channels in Drosophila Circadian Neurons. J Neurosci. 2018;38(42):9059-71. Epub 2018/09/07.
26. Luthi A, McCormick DA. H-current: properties of a neuronal and network pacemaker. Neuron. 1998;21(1):9-12. Epub 1998/08/11.
27. Sheeba V, Gu H, Sharma VK, O'Dowd DK, Holmes TC. Circadian- and light-dependent regulation of resting membrane potential and spontaneous action potential firing of Drosophila circadian pacemaker neurons. Journal of neurophysiology. 2008;99(2):976-88. Epub 2007/12/14.
28. Cao G, Nitabach MN. Circadian control of membrane excitability in Drosophila melanogaster lateral ventral clock neurons. J Neurosci. 2008;28(25):6493-501. Epub 2008/06/20.
29. Muraro NI, Ceriani MF. Acetylcholine from Visual Circuits Modulates the Activity of Arousal Neurons in Drosophila. J Neurosci. 2015;35(50):16315-27. Epub 2015/12/18.
30. Osterwalder T, Yoon KS, White BH, Keshishian H. A conditional tissue-specific transgene expression system using inducible GAL4. Proceedings of the National Academy of Sciences of the United States of America. 2001;98(22):12596-601. Epub 2001/10/25.
31. Depetris-Chauvin A, Berni J, Aranovich EJ, Muraro NI, Beckwith EJ, Ceriani MF. Adult-specific electrical silencing of pacemaker neurons uncouples molecular clock from circadian outputs. Current biology : CB. 2011;21(21):1783-93.
32. Chen Z, Wang Z. Functional study of hyperpolarization activated channel (Ih) in Drosophila behavior. Science China Life sciences. 2012;55(1):2-7. Epub 2012/02/09.
33. Hu W, Wang T, Wang X, Han J. Ih channels control feedback regulation from amacrine cells to photoreceptors. PLoS biology. 2015;13(4):e1002115. Epub 2015/04/02.
34. van den Pol AN. Neuropeptide transmission in brain circuits. Neuron. 2012;76(1):98-115. Epub 2012/10/09.
35. Nusbaum MP, Blitz DM, Marder E. Functional consequences of neuropeptide and small-molecule co-transmission. Nature reviews Neuroscience. 2017;18(7):389-403. Epub 2017/06/09.
36. Helfrich-Forster C. The period clock gene is expressed in central nervous system neurons which also produce a neuropeptide that reveals the projections of circadian pacemaker cells within the brain of

690 Drosophila melanogaster. Proceedings of the National Academy of Sciences of the United States of America.
691 1995;92(2):612-6. Epub 1995/01/17.
692 37. Li MT, Cao LH, Xiao N, Tang M, Deng B, Yang T, et al. Hub-organized parallel circuits of central
693 circadian pacemaker neurons for visual photoentrainment in Drosophila. Nature communications.
694 2018;9(1):4247. Epub 2018/10/14.
695 38. Schlichting M, Menegazzi P, Lelito KR, Yao Z, Buhl E, Dalla Benetta E, et al. A Neural Network
696 Underlying Circadian Entrainment and Photoperiodic Adjustment of Sleep and Activity in Drosophila. J
697 Neurosci. 2016;36(35):9084-96. Epub 2016/09/02.
698 39. Stoleru D, Peng Y, Agosto J, Rosbash M. Coupled oscillators control morning and evening locomotor
699 behaviour of Drosophila. Nature. 2004;431(7010):862-8. Epub 2004/10/16.
700 40. Grima B, Chelot E, Xia R, Rouyer F. Morning and evening peaks of activity rely on different clock
701 neurons of the Drosophila brain. Nature. 2004;431(7010):869-73. Epub 2004/10/16.
702 41. Yao Z, Shafer OT. The Drosophila circadian clock is a variably coupled network of multiple
703 peptidergic units. Science. 2014;343(6178):1516-20. Epub 2014/03/29.
704 42. Park JH, Helfrich-Forster C, Lee G, Liu L, Rosbash M, Hall JC. Differential regulation of circadian
705 pacemaker output by separate clock genes in Drosophila. Proceedings of the National Academy of Sciences
706 of the United States of America. 2000;97(7):3608-13. Epub 2000/03/22.
707 43. Fernandez MP, Berni J, Ceriani MF. Circadian remodeling of neuronal circuits involved in rhythmic
708 behavior. PLoS biology. 2008;6(3):e69. Epub 2008/03/28.
709 44. Gorostiza EA, Depetris-Chauvin A, Frenkel L, Pirez N, Ceriani MF. Circadian Pacemaker Neurons
710 Change Synaptic Contacts across the Day. Current biology : CB. 2014. Epub 2014/08/27.
711 45. Sivachenko A, Li Y, Abruzzi KC, Rosbash M. The transcription factor Mef2 links the Drosophila core
712 clock to Fas2, neuronal morphology, and circadian behavior. Neuron. 2013;79(2):281-92. Epub 2013/07/31.
713 46. Petsakou A, Sapsis TP, Blau J. Circadian Rhythms in Rho1 Activity Regulate Neuronal Plasticity and
714 Network Hierarchy. Cell. 2015;162(4):823-35. Epub 2015/08/04.
715 47. Depetris-Chauvin A, Fernandez-Gamba A, Gorostiza EA, Herrero A, Castano EM, Ceriani MF. Mmp1
716 processing of the PDF neuropeptide regulates circadian structural plasticity of pacemaker neurons. PLoS
717 genetics. 2014;10(10):e1004700. Epub 2014/10/31.
718 48. McGuire SE, Mao Z, Davis RL. Spatiotemporal gene expression targeting with the TARGET and gene-
719 switch systems in Drosophila. Science's STKE : signal transduction knowledge environment.
720 2004;2004(220):pl6. Epub 2004/02/19.
721 49. Chen J, Reiher W, Hermann-Luibl C, Sellami A, Cognigni P, Kondo S, et al. Allatostatin A Signalling in
722 Drosophila Regulates Feeding and Sleep and Is Modulated by PDF. PLoS genetics. 2016;12(9):e1006346.
723 Epub 2016/10/01.
724 50. Guo F, Yu J, Jung HJ, Abruzzi KC, Luo W, Griffith LC, et al. Circadian neuron feedback controls the
725 Drosophila sleep--activity profile. Nature. 2016;536(7616):292-7. Epub 2016/08/02.
726 51. Helfrich-Forster C, Shafer OT, Wulbeck C, Grieshaber E, Rieger D, Taghert P. Development and
727 morphology of the clock-gene-expressing lateral neurons of Drosophila melanogaster. The Journal of
728 comparative neurology. 2007;500(1):47-70. Epub 2006/11/14.
729 52. Noma A, Irisawa H. Membrane currents in the rabbit sinoatrial node cell as studied by the double
730 microelectrode method. Pflugers Archiv : European journal of physiology. 1976;364(1):45-52. Epub
731 1976/06/29.
732 53. He C, Chen F, Li B, Hu Z. Neurophysiology of HCN channels: from cellular functions to multiple
733 regulations. Progress in neurobiology. 2014;112:1-23. Epub 2013/11/05.
734 54. Marx T, Gisselmann G, Stortkuhl KF, Hovemann BT, Hatt H. Molecular cloning of a putative voltage-
735 and cyclic nucleotide-gated ion channel present in the antennae and eyes of Drosophila melanogaster.
736 Invertebrate neuroscience : IN. 1999;4(1):55-63. Epub 2002/12/20.
737 55. Gisselmann G, Gamerschlag B, Sonnenfeld R, Marx T, Neuhaus EM, Wetzel CH, et al. Variants of the
738 Drosophila melanogaster Ih-channel are generated by different splicing. Insect biochemistry and molecular
739 biology. 2005;35(5):505-14. Epub 2005/04/05.
740 56. Jackson HA, Marshall CR, Accili EA. Evolution and structural diversification of hyperpolarization-
741 activated cyclic nucleotide-gated channel genes. Physiological genomics. 2007;29(3):231-45. Epub
742 2007/01/18.

743 57. Ishii TM, Nakashima N, Takatsuka K, Ohmori H. Peripheral N- and C-terminal domains determine
744 deactivation kinetics of HCN channels. Biochemical and biophysical research communications.
745 2007;359(3):592-8. Epub 2007/06/06.
746 58. Hegle AP, Frank CA, Berndt A, Klose M, Allan DW, Accili EA. The Ih Channel Gene Promotes Synaptic
747 Transmission and Coordinated Movement in Drosophila melanogaster. Frontiers in molecular neuroscience.
748 2017;10:41. Epub 2017/03/14.
749 59. Gonzalo-Gomez A, Turiegano E, Leon Y, Molina I, Torroja L, Canal I. Ih current is necessary to
750 maintain normal dopamine fluctuations and sleep consolidation in Drosophila. PloS one. 2012;7(5):e36477.
751 Epub 2012/05/11.
752 60. Allebrandt KV, Teder-Laving M, Cusumano P, Frishman G, Levandovski R, Ruepp A, et al. Identifying
753 pathways modulating sleep duration: from genomics to transcriptomics. Scientific reports. 2017;7(1):4555.
754 Epub 2017/07/06.
755 61. Colwell CS. Linking neural activity and molecular oscillations in the SCN. Nature reviews
756 Neuroscience. 2011;12(10):553-69.
757 62. Notomi T, Shigemoto R. Immunohistochemical localization of Ih channel subunits, HCN1-4, in the
758 rat brain. The Journal of comparative neurology. 2004;471(3):241-76. Epub 2004/03/03.
759 63. de Jeu MT, Pennartz CM. Functional characterization of the H-current in SCN neurons in subjective
760 day and night: a whole-cell patch-clamp study in acutely prepared brain slices. Brain research.
761 1997;767(1):72-80. Epub 1997/08/29.
762 64. O'Neill JS, Maywood ES, Chesham JE, Takahashi JS, Hastings MH. cAMP-dependent signaling as a
763 core component of the mammalian circadian pacemaker. Science. 2008;320(5878):949-53. Epub
764 2008/05/20.
765 65. Atkinson SE, Maywood ES, Chesham JE, Wozny C, Colwell CS, Hastings MH, et al. Cyclic AMP
766 signaling control of action potential firing rate and molecular circadian pacemaking in the suprachiasmatic
767 nucleus. Journal of biological rhythms. 2011;26(3):210-20. Epub 2011/06/02.
768 66. Duvall LB, Taghert PH. E and M circadian pacemaker neurons use different PDF receptor
769 signalosome components in drosophila. Journal of biological rhythms. 2013;28(4):239-48. Epub 2013/08/10.
770 67. Sabado V, Vienne L, Nunes JM, Rosbash M, Nagoshi E. Fluorescence circadian imaging reveals a
771 PDF-dependent transcriptional regulation of the Drosophila molecular clock. Scientific reports.
772 2017;7:41560. Epub 2017/01/31.
773 68. Seluzicki A, Flourakis M, Kula-Eversole E, Zhang L, Kilman V, Allada R. Dual PDF signaling pathways
774 reset clocks via TIMELESS and acutely excite target neurons to control circadian behavior. PLoS biology.
775 2014;12(3):e1001810. Epub 2014/03/20.
776 69. Yamada R, Kuba H, Ishii TM, Ohmori H. Hyperpolarization-activated cyclic nucleotide-gated cation
777 channels regulate auditory coincidence detection in nucleus laminaris of the chick. J Neurosci.
778 2005;25(39):8867-77. Epub 2005/09/30.
779 70. Pavlov I, Scimemi A, Savtchenko L, Kullmann DM, Walker MC. I(h)-mediated depolarization
780 enhances the temporal precision of neuronal integration. Nature communications. 2011;2:199. Epub
781 2011/02/18.
782 71. Baumann VJ, Lehnert S, Leibold C, Koch U. Tonotopic organization of the hyperpolarization-
783 activated current (Ih) in the mammalian medial superior olive. Frontiers in neural circuits. 2013;7:117. Epub
784 2013/07/23.
785 72. Sun QQ, Prince DA, Huguenard JR. Vasoactive intestinal polypeptide and pituitary adenylate
786 cyclase-activating polypeptide activate hyperpolarization-activated cationic current and depolarize
787 thalamocortical neurons in vitro. J Neurosci. 2003;23(7):2751-8. Epub 2003/04/10.
788 73. Abruzzi KC, Rodriguez J, Menet JS, Desrochers J, Zadina A, Luo W, et al. Drosophila CLOCK target
789 gene characterization: implications for circadian tissue-specific gene expression. Genes & development.
790 2011;25(22):2374-86. Epub 2011/11/17.
791 74. DiFrancesco JC, DiFrancesco D. Dysfunctional HCN ion channels in neurological diseases. Frontiers
792 in cellular neuroscience. 2015;6:174. Epub 2015/03/26.
793 75. Brennan GP, Baram TZ, Poolos NP. Hyperpolarization-Activated Cyclic Nucleotide-Gated (HCN)
794 Channels in Epilepsy. Cold Spring Harbor perspectives in medicine. 2016;6(3):a022384. Epub 2016/03/05.

795 76. Ku SM, Han MH. HCN Channel Targets for Novel Antidepressant Treatment. Neurotherapeutics : the
796 journal of the American Society for Experimental NeuroTherapeutics. 2017;14(3):698-715. Epub
797 2017/06/01.
798 77. McGuire SE, Roman G, Davis RL. Gene expression systems in Drosophila: a synthesis of time and
799 space. Trends in genetics : TIG. 2004;20(8):384-91. Epub 2004/07/21.
800 78. Hendricks JC, Finn SM, Panckeri KA, Chavkin J, Williams JA, Sehgal A, et al. Rest in Drosophila is a
801 sleep-like state. Neuron. 2000;25(1):129-38. Epub 2000/03/09.
802 79. Shaw PJ, Cirelli C, Greenspan RJ, Tononi G. Correlates of sleep and waking in Drosophila
803 melanogaster. Science. 2000;287(5459):1834-7. Epub 2000/03/10.
804 80. Geissmann Q, Garcia Rodriguez L, Beckwith EJ, Gilestro GF. Rethomics: An R framework to analyse
805 high-throughput behavioural data. PloS one. 2019;14(1):e0209331. Epub 2019/01/17.
806 81. Dietzl G, Chen D, Schnorrer F, Su KC, Barinova Y, Fellner M, et al. A genome-wide transgenic RNAi
807 library for conditional gene inactivation in Drosophila. Nature. 2007;448(7150):151-6. Epub 2007/07/13.
808 82. Lin WH, Baines RA. Regulation of membrane excitability: a convergence on voltage-gated sodium
809 conductance. Molecular neurobiology. 2015;51(1):57-67. Epub 2014/03/29.

Gene Symbol	CG	RNAi info	Channel type	tau (h)	Rhythm. (%)	n	N
cac	CG1522	DRSC 27244 + VDRC KK 104168	VG Ca++ channel	**24.48±0.21***	**57±11***	75	5
Ca-α1T	CG15899	VDRC KK 108827	VG Ca++ channel	**24.85±0.14***	**30±9***	70	3
ClC-a	CG31116	VDRC KK 110394	VG Cl- channel	**21.78±0.13*** & 24.25±0.20	**4±4***	37	2
CngA	CG42701	DRSC 26014 + VDRC KK 101745	Cyclic-nucleotide G channel	23.55±0.06	**65±2***	27	2
I_h	CG8585	DRSC 29574 + VDRC KK 110274	VG cation channel	23.95±0.03	**74±8***	40	3
Ork1	CG1615	DRSC 25885 + VDRC KK 104883	K+ leak channel	**25.00±0.46***	**48±12***	33	3
Shal	CG9262	NIG 9262R-3	VG K+ channel	**24.59±0.11***	89±6	59	4
tipE	CG1232	NIG 1232R-3	VG Na+ auxiliary subunit	**25.73±0.40***	85±12	46	3
tipE	CG1232	DRSC 26249	VG Na+ auxiliary subunit	**25.60±0.38***	**48±16***	47	3

Table 1: Positive hits of the ion channel downregulation behavioral screen.
This table includes a list of genes that, when downregulated exclusively in LNvs using these particular RNAi constructs, produced statistically significant alterations in free running period and/or percentage of rhythmicity. Values represent the average of mean values of N independent experiments ± SEM. n indicates total number of individuals tested. *Indicates statistically significant difference ($p<0.05$) after a one-way ANOVA comparing *pdf,dicer*>RNAi to control genotypes *pdf,dicer*/+ (average period 24.00±0.07h and average rhythmicity 95±3%) and RNAi/+ (average period 24.08±0.17h and average rhythmicity 93±4%). Tukey test was used for means comparison and Levene's test for checking ANOVA assumption of homogeneity of variance. In the case where information for two RNAi constructs is given, it means that each RNAi on its own did not show significant differences compared to controls, but did show a trend towards an altered phenotype. For that reason two different RNAis for the same gene were genetically combined to achieve added downregulation strength. In the case of *ClC-a*, the reduction of rhythmicity was due to the appearance of complex rhythms and not to the deconsolidation of locomotor activity organization; the tau of each component of complex rhythms is given. V: Voltage, G: Gated, DRSC: *Drosophila* RNAi Screening Center, VDRC: Vienna *Drosophila* Resource Center, NIG: National Institute of Genetics.

	DD Analysis				LD Analysis			
Genotype	**tau (h)**	**Rhythm.(%)**	**n**	**N**	**MAI**	**EAI**	**n**	**N**
pdf,dicer/+	24.00±0.07	95±3	75	3	0.73±0.02	0.88± 0.02	55	2
UAS-I_h^{RNAi}/+	23.71±0.02	92±6	39		0.77±0.03	0.80±0.03	21	
pdf,dicer>UAS-I_h^{RNAi}	23.95±0.03	**74±8***	40		0.67±0.03	0.80±0.02	23	
pdfGS/+ , RU	24.59±0.41	97±2	64	3	0.64±0.01	**0.66±0.02***	76	3
UAS-I_h^{RNAi}/+ , RU	23.75±0.06	100±0	41		0.72±0.02	0.58±0.01	50	
pdfGS>UAS-I_h^{RNAi} , RU	24.81±0.75	**57±12***	67		**0.59±0.01***	0.60±0.01	74	
control	24.02±0.05	96±2	86	4	0.68±0.03	0.84±0.02	62	2
I_h^{f01485}/+	23.87±0.03	96±3	80		0.71±0.04	0.89±0.02	32	
I_h^{f01485}	23.56±0.05	**60±3***	98		0.55±0.05	**0.65±0.03***	34	
I_h^{f03355}/+	23.86±0.05	99±1	96		0.73±0.03	0.92± 0.02	30	
I_h^{f03355}	23.88±0.08	**39±12***	104		**0.51±0.03***	**0.67±0.03***	30	

Table 2: I_h genetic manipulations disrupt circadian locomotor activity organization.

DD Analysis (left): the average free running period and percentage of rhythmicity of populations of male flies of the indicated genotypes are shown. Values represent the average of N independent experiments ± SEM. n indicates total number of individuals tested. *Indicates statistically significant difference ($p<0.05$) after a one-way ANOVA comparing experimental genotypes to genetic controls. UAS-I_h^{RNAi} refers to the genetic combination of two UAS-I_h^{RNAi} constructs: DRSC 29574 + VDRC KK 110274 mentioned in Table 1). In the case of the I_h null mutants, I_h^{f01485} and I_h^{f03355}, homozygotes were compared to a w^{1118} control and to heterozygotes (I_h^{f03355} crossed by w^{1118}). RU refers to the presence of the steroid RU486 (200 µg/ml), the activator of the GeneSwitch system, in the food media. LD Analysis (right): Morning Anticipation Index (MAI) and Evening Anticipation Index (EAI) were calculated for the same genotypes. *Indicates statistically significant difference ($p<0.05$) after Kruskal-Wallis statistical analysis with Dunn's multiple comparisons test.

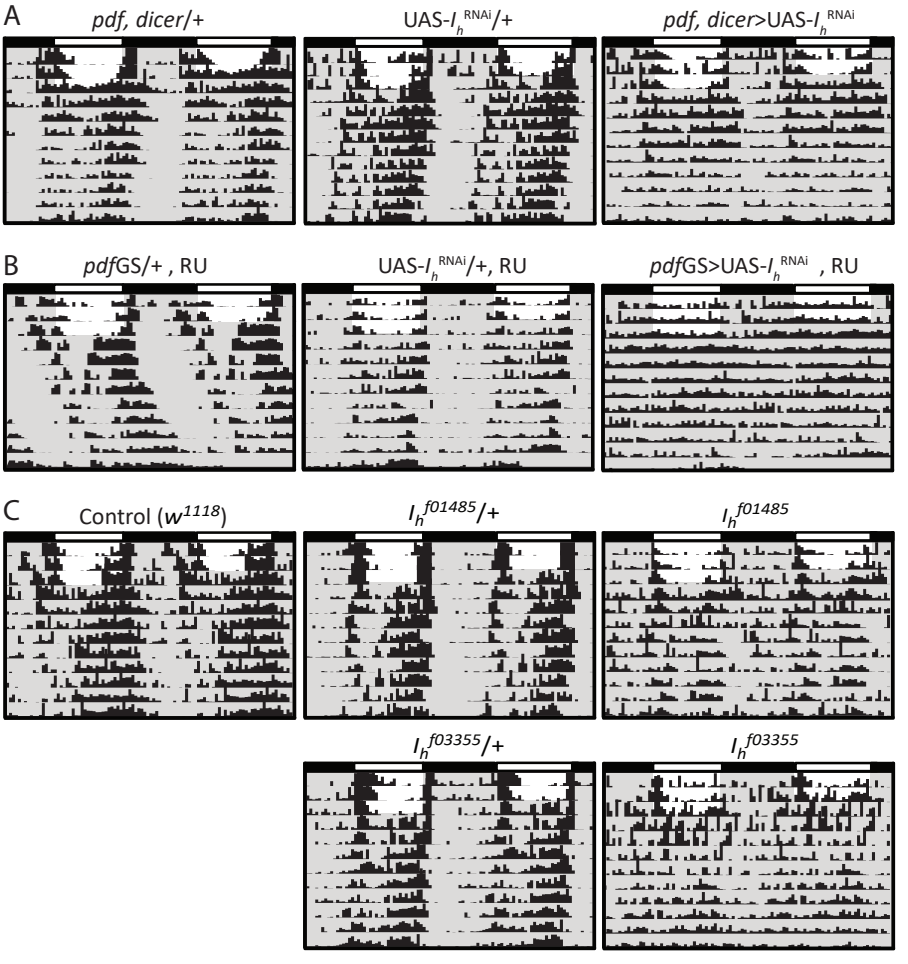

Fig 1: I_h genetic manipulations disrupt circadian locomotor activity organization. Representative double-plotted actograms of the different I_h genetic manipulations tested. **A)** LNvs constitutive downregulation of I_h using *pdf*,dicer and UAS-I_h^{RNAi} (in all cases UAS-I_h^{RNAi} refers to the genetic combination of two UAS-I_h^{RNAi} constructs: DRSC 29574 + VDRC KK 110274 mentioned in Table 1) and genetic controls. **B)** LNvs acute downregulation of I_h using pdfGS and UAS-I_h^{RNAi} and genetic controls. RU refers to the presence of the steroid RU486, the activator of the GeneSwitch system, in the food media. **C)** Homozygote I_h null mutants, I_h^{f01485} and I_h^{f03355}, and controls (w^{1118} and heterozygote mutants, crossed by w^{1118}). In the case of the experimental genotypes an actogram of an arrhythmic individual is shown, different genetic manipulations varied in the degree of arrhythmicity (see Table 2). No statistically significant alterations in free running period were found for these genetic manipulations.

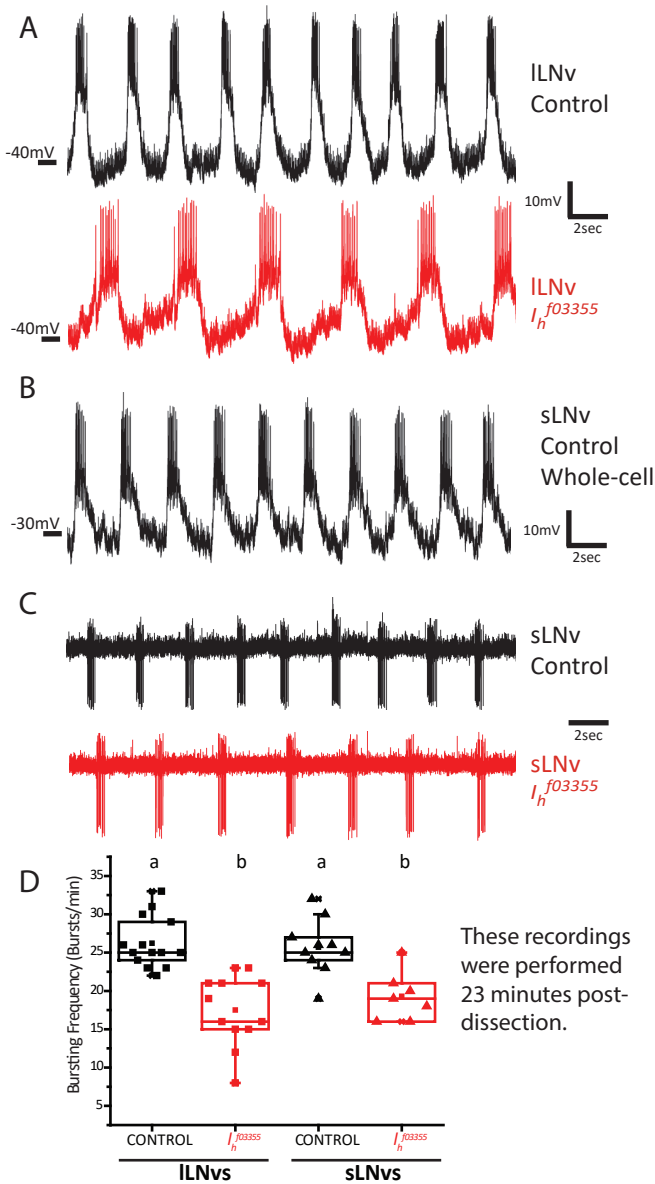

Fig 2: I_h is important for high frequency bursting of LNvs.
A) Representative traces of whole-cell patch clamp recordings of lLNvs of control (*pdf*-RFP, top) and I_h homozygote mutant genotypes (I_h^{f03355}; *pdf*-RFP, bottom). **B)** Representative trace of a recording of a sLNv control (*pdf*-RFP) in whole-cell patch clamp configuration. **C)** Representative traces of cell-attached recordings of sLNvs of control (pdf-RFP, top) and I_h homozygote mutant genotypes (I_h^{f03355}; *pdf*-RFP, bottom). **D)** Box plot showing bursting frequency quantification of lLNvs and sLNvs of control (*pdf*-RFP) and I_h homozygote mutant genotypes (I_h^{f03355}; *pdf*-RFP). All quantifications were done at exactly 23min post-dissection. Different letters indicate significant differences ($p<0.05$) after a one-way ANOVA with Tukey test for means comparisons. n: $lLNvs_{CONTROL}$=14, $lLNvs_{lhf03355}$=12, $sLNvs^{CONTROL}$=10, $sLNvs_{lhf03355}$=7.

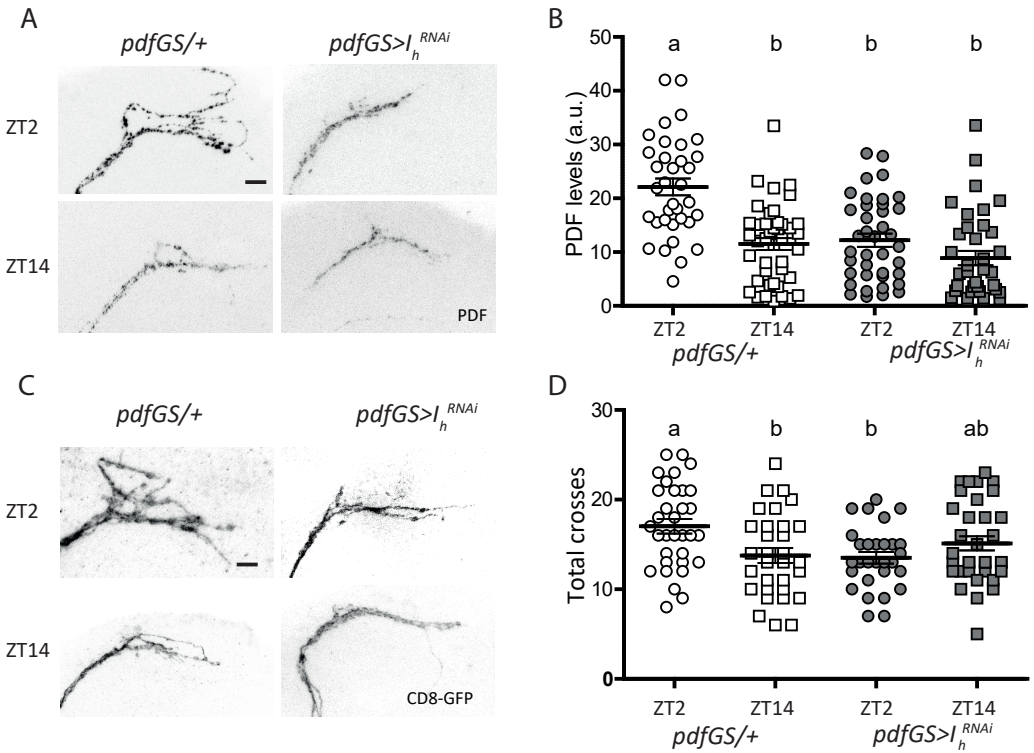

Fig 3: I_h downregulation affects PDF levels and structural plasticity.
A) Confocal images of representative sLNvs dorsal projections of individual flies of control (*pdf*GS/+) and I_h downregulation (*pdf*GS>I_h^{RNAi}) at day (top) and night (bottom) showing their PDF content. Flies were kept in LD 12:12 at 25°C for 7 days in food containing RU486. Brains were dissected at ZT02 and ZT14 and standard anti-PDF immunofluorescence detection was performed. The bar indicates 10µm. **B)** PDF quantitation of the sLNvs dorsal projections for the four conditions mentioned before. Circles represent day time, squares, night time; empty symbols are the control genotype (*pdf*GS/+) and filled symbols, the experimental one (*pdf*GS>I_h^{RNAi}). Different letters indicate significant differences, analysis included a two-way ANOVA (genotype and time of day) [$F_{(3,150)}$=18.58 p<0.0001 with Tukey post hoc test, α =0.05], n=35-43 per group. **C)** Confocal images of sLNvs projections illustrating their complexity at ZT02 and ZT14 for both in the control and I_h downregulated genotypes. Procedure as in A but with immunofluorescence against GFP. The bar indicates 10µm. **D)** Complexity quantitation was asses by Sholl analysis (ImageJ) corroborated by visual inspection of each picture. Symbols as in B, analysis included a two-way ANOVA [$F_{(3,123)}$=4.24 p<0.01 with Tukey post hoc test, α =0.05]. Different letters indicate significant differences. n=34-38 per group.

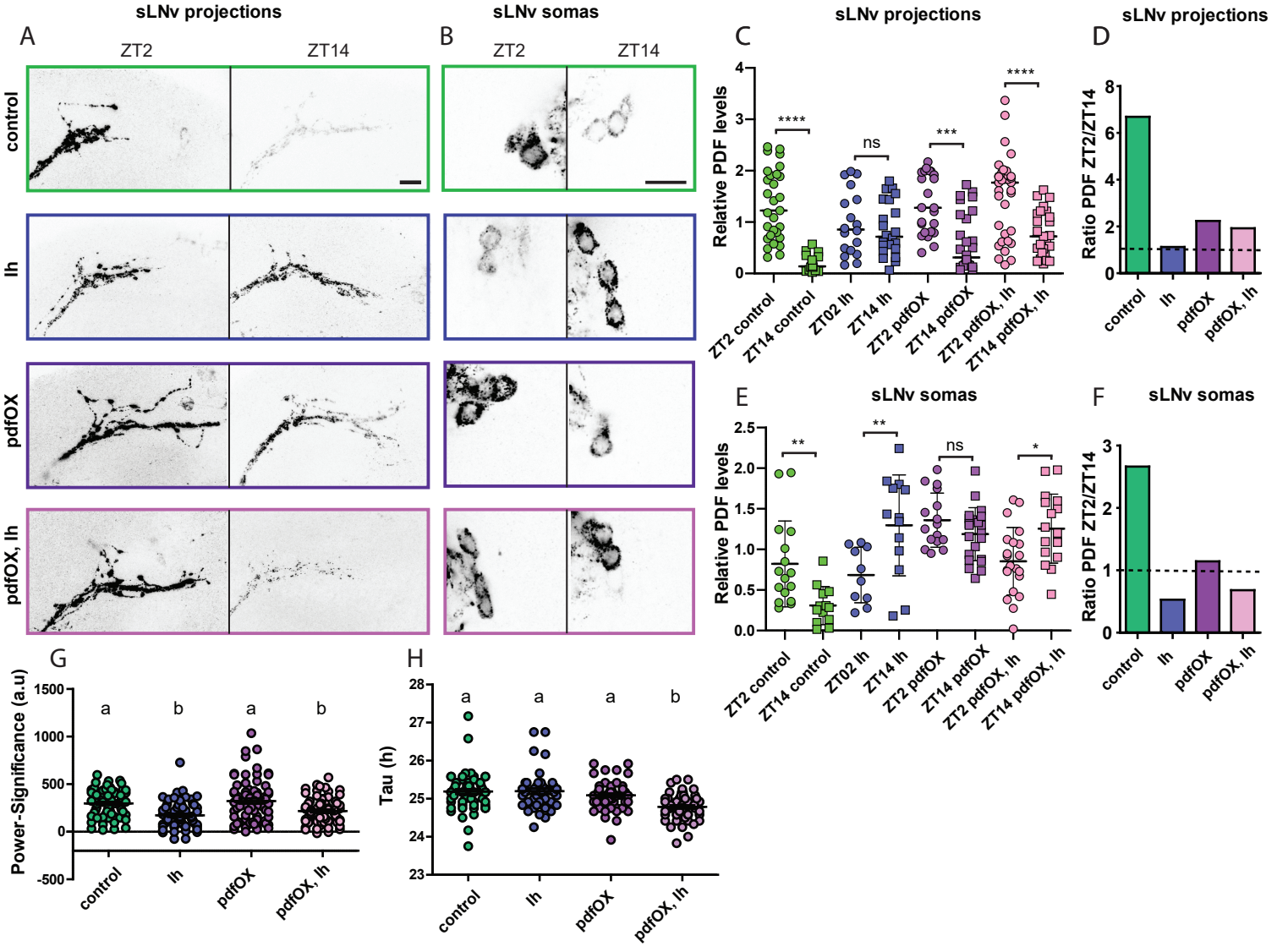

Fig 4: PDF transport is affected upon I_h manipulation.

A, B) Confocal images of representative sLNv projections (A) and somas (B) of individual flies of *pdf*GS/+ (control), *pdf*GS>I_h^{RNAi} (I_h), *pdf*GS>UAS-*pdf* (*pdf*OX) and *pdf*GS>UAS-*pdf* , I_h^{RNAi} (*pdf*OX, I_h) at day (left) and night (right) showing their PDF content. Flies were kept in LD 12:12 at 25°C for 7 days in food containing RU486. Brains were dissected at ZT02 and ZT14 and standard anti-PDF immunofluorescence detection was performed, bars indicate 10µm. **C, E)** PDF quantitation of the sLNv dorsal projections (C) or somas (E) for the four genotypes mentioned before. Circles represent day time, squares, night time; each color is a different genotype. Asterisks represent significant statistical differences. For the projections, a non-parametric ANOVA Kruskal-Wallis test and Dunn's comparisons test showed differences among the two time points in control, *pdf*OX and *pdf*OX, I_h groups but not in I_h group [Kruskal-Wallis statistic (8,196)=71.95, p<0.0001, n=18-28]. Immunoreactivity from somas was analyzed with one-way ANOVA and Sidak's multiple comparisons test and revealed differences between the two time-points in every genotype except *pdf*OX, although I_h and *pdf*OX, I_h showed differences in the anti-phase direction compared to the control, ANOVA F(7, 120)=10.95, p<0.0001, n=10-22 (each point is the average of 3-4 cell somas for one hemi-brain of an individual fly). **D, F)** Morning to evening PDF level ratios for axonal projections (D) or somas (F). **G)** Locomotor behavior under constant darkness of the same genotypes as before. Experiments were performed as in Fig 1 and Table 2. The rhythmicity measured as power-significance was analyzed by Kruskal-Wallis test followed by Dunn's comparisons test and showed a significant reduction of power-significance in I_h and *pdf*OX, I_h compared to control and *pdf*OX as indicated by different letters [Kruskal-Wallis statistic (4,31)=31.40, p<0.0001, n=65-72]. **H)** Free running period values were analyzed as well. The same type of analysis reveals a reduction of tau in *pdf*OX, I_h compared to all the other genotypes as indicated by a different letter [Kruskal-Wallis statistic (4,31)=38.28, p<0.0001, n=45-58].

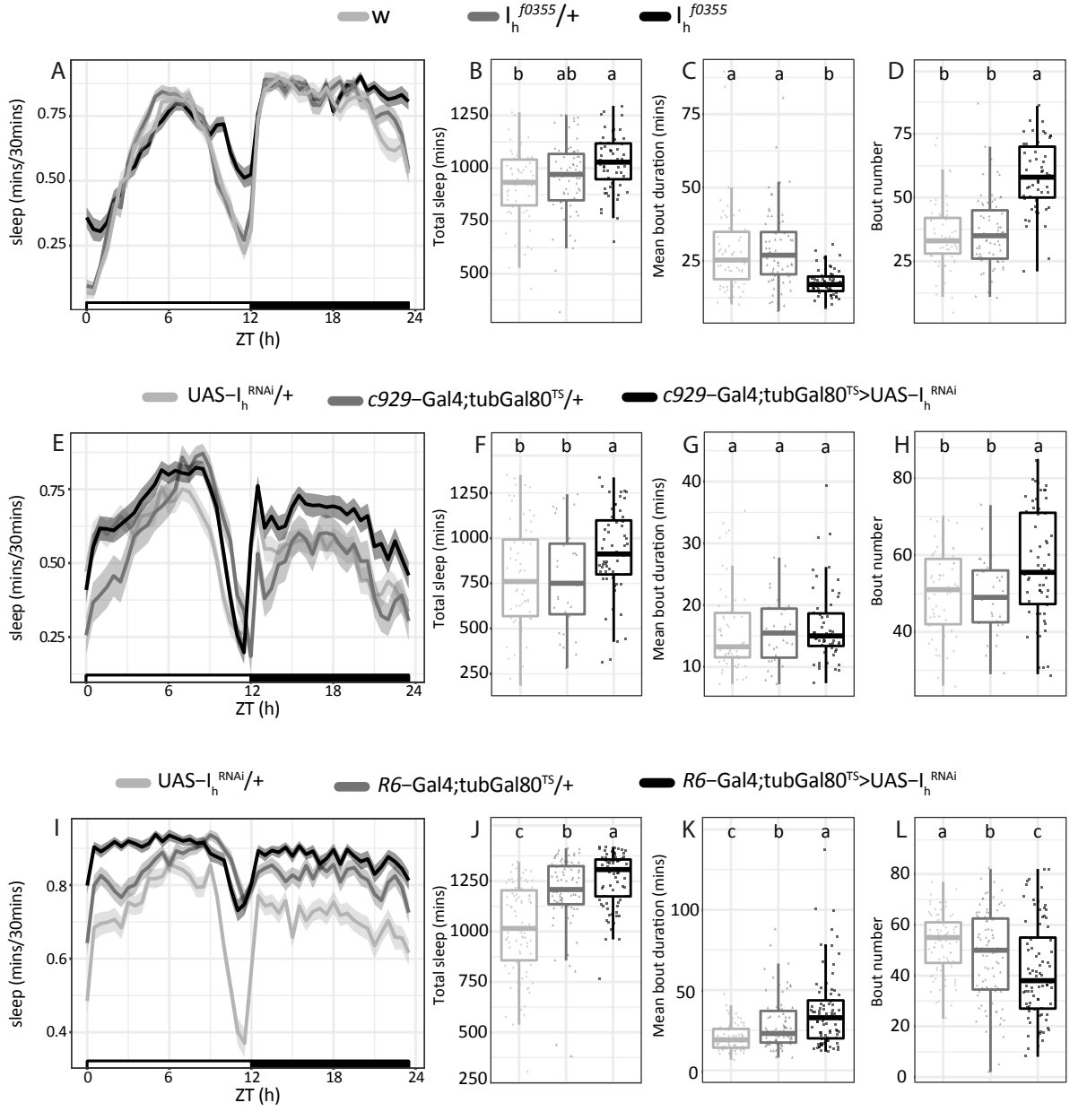

Fig 5: Genetic manipulations of I_h increase sleep.

A, E, I) Sleep ethograms for the indicated genotypes, quantification of the relative amount of sleep every 30 minutes as a function of the time of the day (starting at zeitgeber time = 0, when lights are turned on) and its standard deviation (shadowed area). Black and white bars at the bottom represent daytime (white) and nighttime (black). **B, F, J)** Boxplots showing the total amount of sleep minutes for each genotype. **C, G, K)** Boxplots showing the average duration of sleep episodes for each genotype. **D, H, L)** Boxplots showing the total amount of sleep episodes for each genotype. For all the boxplots, different letters indicate significant differences ($p<0.05$) after non parametric Kruskal-Wallis statistical analysis with multiple comparisons (p adjustment method= BH). For more information on sleep parameters see Table 3.

Genotype	Total Sleep (min)	Daytime Sleep (min)	Nighttime Sleep (min)	Bout Duration (min)	Sleep Bout number	Latency lights on (min)	Latency lights off (min)	Activity Index	n	N
I_h^{f0355}	**1026.6 ± 17.8 [a]**	430.0 ± 14.3 [a]	**599.9 ± 8.4 [a]**	**17.6 ± 0.6 [b]**	**58.5 ± 1.8 [a]**	**25.0 ± 5.8 [b]**	**15.3 ± 1.9 [b]**	**4.24 ± 0.18 [a]**	56	
I_h^{f0355}/+	956.9 ± 21.6 [ab]	394.6 ± 11.8 [a]	560.5 ± 15.0 [ab]	29.0 ± 1.6 [a]	36.4 ± 1.7 [b]	71.5 ± 6.3 [a]	27.1 ± 3.7 [a]	2.18 ± 0.08 [b]	69	3
w^{1118}	922.2 ± 20.8 [b]	380.5 ± 12.6 [a]	533.4 ± 17.4 [b]	28.4 ± 1.7 [a]	35.3 ± 1.6 [b]	78.7 ± 7.3 [a]	27.6 ± 3.0 [a]	2.02 ± 0.05 [b]	66	
c929-Gal4;*tub*-Gal80^{TS}>UAS-I_h^{RNAi}	**921.7 ± 31.6 [a]**	464.1 ± 16.1 [a]	**457.7 ± 21.6 [a]**	17.0 ± 0.9 [a]	**57.5 ± 1.9 [a]**	18.1 ± 3.1 [a]	15.9 ± 2.7 [b]	2.16 ± 0.07 [b]	58	
c929-Gal4;*tub*-Gal80^{TS}/+	773.0 ± 50.7 [b]	432.6 ± 25.5 [a]	340.4 ± 30.3 [b]	15.7 ± 0.9 [a]	49.4 ± 1.8 [b]	51.0 ± 12.0 [a]	45.7 ± 8.1 [a]	1.88 ± 0.05 [c]	31	2
UAS-I_h^{RNAi}/+	793.5 ± 38.1 [b]	424.8 ± 21.5 [a]	368.7 ± 21.1 [b]	16.0 ± 0.8 [a]	50.6 ± 1.4 [b]	25.5 ± 7.5 [a]	17.4 ± 2.9 [b]	2.52 ± 0.09 [a]	61	
R6-Gal4;*tub*-Gal80^{TS}>UAS-I_h^{RNAi}	**1264.9 ± 14.2 [a]**	**636.7 ± 7.6 [a]**	**630.7 ± 21.6 [a]**	**37.1 ± 2.5 [a]**	**41.7 ± 2.0 [c]**	**2.2 ± 0.7 [c]**	16.8 ± 3.7 [b]	**2.63 ± 0.08 [a]**	85	
R6-Gal4;*tub*-Gal80^{TS}/+	1195.6 ± 19.6 [b]	605.9 ± 10.8 [b]	589.6 ± 30.3 [b]	31.2 ± 3.1 [b]	47.3 ± 1.9 [b]	5.4 ± 1.1 [b]	24.7 ± 6.2 [b]	2.16 ± 0.06 [b]	87	3
UAS-I_h^{RNAi}/+	1015.7 ± 23.7 [c]	515.0 ± 12.8 [c]	504.6 ±21.1 [c]	20.5 ± 0.8 [c]	52.5 ± 1.2 [a]	13.6 ± 2.8 [a]	18.2 ± 2.4 [a]	2.21 ± 0.08 [b]	89	
pdf-Gal4, UAS-*dicer2*;*tub*-Gal80^{TS}>UAS-I_h^{RNAi}	**955.9 ± 27.8 [a]**	603.5 ± 12.3 [ab]	**357.7 ± 20.5 [a]**	25.8 ± 1.1 [b]	39.2 ± 1.6 [a]	17.2 ± 3.3 [b]	**19.4 ± 4.6 [b]**	1.82 ± 0.03 [a]	61	
pdf-Gal4, UAS-dicer2;*tub*-Gal80^{TS}/+	847.9 ± 15.7 [b]	632.4 ± 7.4 [a]	215.5 ± 12.5 [c]	30.1 ± 1.0 [a]	30.0 ± 1.8 [b]	22.5 ± 1.7 [a]	36.5 ± 5.6 [a]	1.64 ± 0.03 [b]	63	2
UAS-I_h^{RNAi}/+	848.7 ± 20.0 [b]	573.1 ± 12.9 [b]	274.9 ± 15.6 [b]	22.4 ± 1.1 [c]	41.9 ± 1.7 [a]	14.8 ± 1.9 [b]	24.5 ± 3.8 [a]	1.81 ± 0.03 [a]	61	
c929-Gal4>UAS-I_h^{RNAi}	980.5 ± 29.9 [a]	**496.1 ± 15.0 [a]**	484.1 ± 17.2 [a]	18.2 ± 1.3 [a]	60.3 ± 2.1 [a]	**8.6 ± 2.4 [c]**	21.7 ± 2.6 [b]	**1.98 ± 0.04 [a]**	72	
c929-Gal4/+	793.1 ± 26.8 [b]	394.4 ± 13.5 [c]	401.4 ± 17.1 [b]	15.5 ± 0.9 [a]	52.7 ± 1.5 [b]	56.5 ± 7.7 [a]	32.3 ± 3.0 [a]	1.89 ± 0.03 [ab]	71	3
UAS-I_h^{RNAi}/+	919.0 ± 29.5 [a]	444.5 ± 15.9 [b]	474.9 ± 17.3 [a]	16.9 ± 1.1 [a]	58.7 ± 1.6 [a]	19.9 ± 4.0 [b]	26.5 ± 5.1 [b]	1.80 ± 0.03 [b]	70	
R6-Gal4>UAS-I_h^{RNAi}	**1111.7 ± 27.7 [a]**	**545.9 ± 15.7 [a]**	**551.2 ± 14.9 [a]**	**27.2 ± 0.6 [a]**	53.3 ± 2.9 [a]	**6.8 ± 2.6 [b]**	30.9 ± 7.2 [a]	2.21 ± 0.09 [a]	65	
R6-Gal4/+	854.5 ± 35.9 [b]	409.7 ± 18.0 [b]	440.9 ± 20.8 [b]	15.6 ± 1.2 [b]	58.2 ± 2.3 [a]	19.0 ± 3.0 [a]	26.6 ± 4.4 [a]	2.06 ± 0.03 [a]	71	3
UAS-I_h^{RNAi}/+	826.9 ± 28.1 [b]	400.6 ± 16.4 [b]	423.6 ± 15.5 [b]	14.1 ± 2.9 [b]	59.9 ± 1.4 [a]	32.9 ± 5.4 [a]	24.2 ± 2.5 [a]	1.81 ± 0.03 [b]	70	
pdf-Gal4, UAS-dicer2>UAS-I_h^{RNAi}	715.9 ± 37.8 [b]	330.6 ± 20.7 [b]	385.3 ± 21.6 [b]	14.3 ± 0.9 [b]	52.2 ± 1.9 [a]	27.5 ± 6.2 [b]	36.5 ± 6.2 [a]	1.75 ± 0.04 [b]	64	
pdf-Gal4, UAS-dicer2/+	714.0 ± 29.3 [b]	320.8 ± 15.3 [b]	393.3 ± 18.3 [b]	14.0 ± 0.7 [b]	52.4 ± 1.6 [a]	70.0 ± 7.1 [a]	42.4 ± 6.3 [a]	1.73 ± 0.03 [b]	56	2
UAS-I_h^{RNAi}/+	937.5 ± 28.1 [a]	414.3 ± 18.4 [a]	525.5 ± 15.2 [a]	18.7 ± 0.9 [a]	52.6 ± 1.7 [a]	39.0 ± 6.5 [b]	21.3 ± 4.6 [b]	1.89 ± 0.03 [a]	64	

Table 3: Sleep parameters after genetic manipulation of I_h.

The following sleep parameters upon the different genetic manipulations presented in the first column are shown; total sleep, daytime sleep, nighttime sleep, sleep bout duration, bout amount, latency to lights on, latency to lights off, and activity index (defined as the average activity counts in the active minutes). Average ± SEM (Standard Error of the Mean) of N experiments using a final n number of individuals are displayed. Different letters indicate significant differences ($p<0.05$) after non parametric Kruskal-Wallis statistical analysis with multiple comparisons (p adjustment method= BH). Sleep parameters where the experimental genotype showed statistically significant differences compared to genetic controls are displayed in bold.

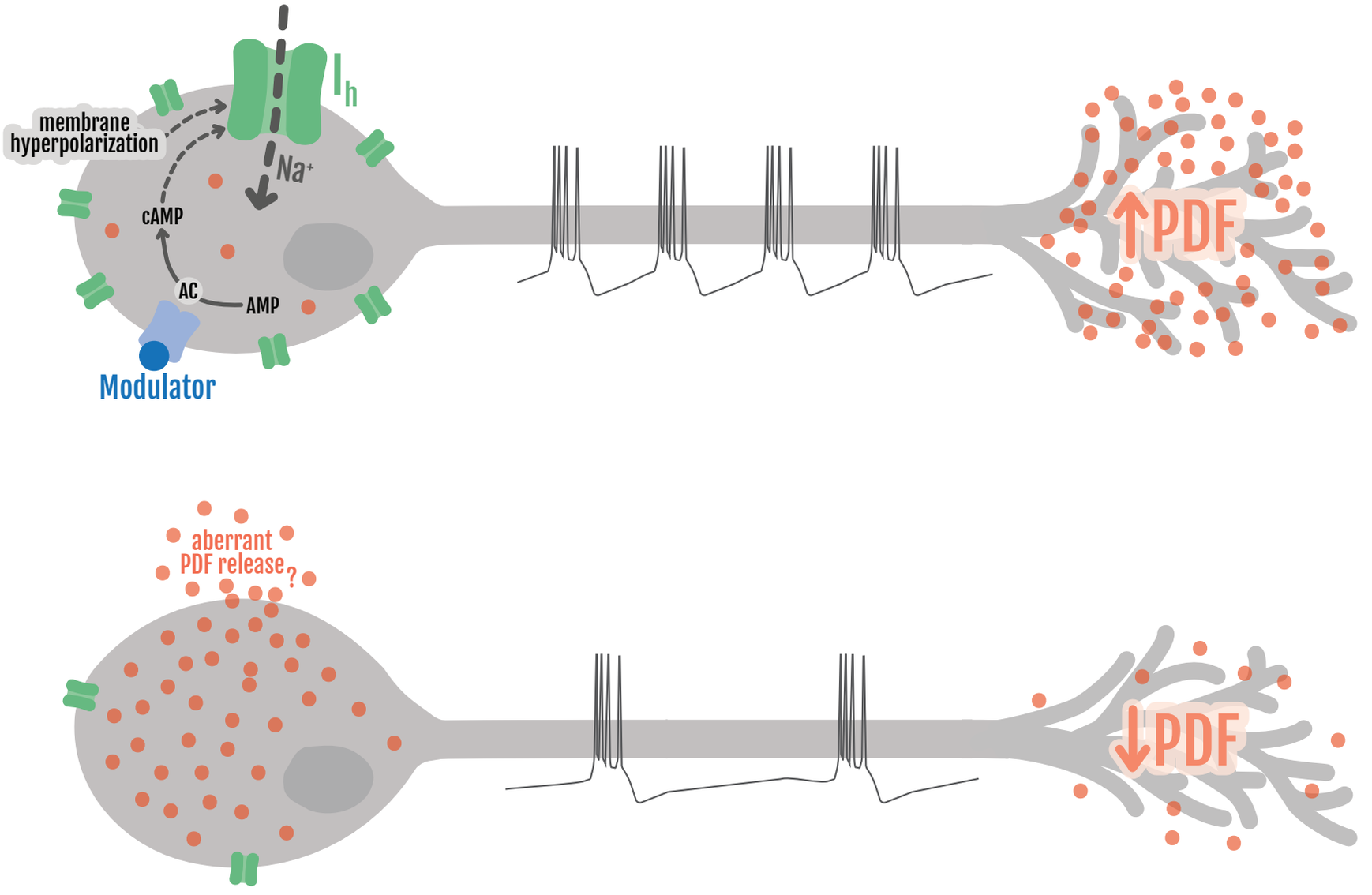

Fig 6: Model summarizing the findings reported and the hypotheses raised by this work.
I_h channel (in green) responds to membrane hyperpolarization and is modulated by cyclic nucleotides, serving as coincidence detector for electrical and chemical signals mediated by ligands that activate G protein-coupled receptors (such as PDF, Dopamine or other neuropeptides, symbolized by "Modulator", in blue). I_h function is necessary to allow LNvs to fire action potentials in a high frequency bursting mode, which permits the release of PDF (in orange) at high levels and in a timely manner (top neuron). In the absence or upon I_h knock down (bottom neuron), bursting does not reach such high frequency and PDF levels at the axonal projections are reduced. Associated to the decreased bursting frequency, large quantities of PDF accumulate at the soma, likely due to a failure in dense core vesicle transport. This may give rise to a hypothetical aberrant PDF release from the overloaded soma, likely overriding the internal temporal control. All in all, these cellular disruptions result in anomalies at the behavioral level, such as disorganization of circadian locomotor activity and an increase in sleep. At the level of the axonal projections, the model represents an early daytime situation, where in control animals PDF levels are high and the axonal terminal are spread out. However, the accumulation and possible aberrant release of PDF from the soma is more likely to happen during the night (see Fig 4).